Molecular Neurobiology (2019) 56:7534–7556
https://doi.org/10.1007/s12035-019-1590-6

Running-Activated Neural Stem Cells Enhance Subventricular Neurogenesis and Improve Olfactory Behavior in p21 Knockout Mice

Vittoria Nicolis di Robilant[1] · Raffaella Scardigli[2] · Georgios Strimpakos[1] · Felice Tirone[1] · Silvia Middei[1] · Chiara Scopa[2] · Marco De Bardi[3] · Luca Battistini[3] · Daniele Saraulli[1] · Stefano Farioli Vecchioli[1]

Received: 21 January 2019 / Accepted: 27 March 2019 / Published online: 6 May 2019

Abstract

In the subventricular zone (SVZ) of the adult brain, the neural stem cells (NSCs) ensure a continuous supply of new neurons to the olfactory bulb (OB), playing a key role in its plasticity and olfactory-related behavior. The activation and expansion of NSCs within the SVZ are finely regulated by environmental and intrinsic factors. Running represents one of the most powerful neurogenic stimuli, although is ineffective in enhancing SVZ neurogenesis. The cell cycle inhibitor p21 is an intrinsic inhibitor of NSCs' expansion through the maintenance of their quiescence and the restrain of neural progenitor proliferation. In this work, we decided to test whether running unveils the intrinsic neurogenic potential of p21-lacking NSCs. To test this hypothesis, we examined the effect of three different paradigms of voluntary running (5, 12, and 21 days) on SVZ neurogenesis of p21 knockout (KO) male mice at two different stages of development, 2 and 12 months of age. In vivo and in vitro data clearly demonstrate that physical activity is consistent with the activation and expansion of NSCs and with the enhancement of SVZ neurogenesis in p21 KO mice. We also found that 12 days of running contribute to the increase in the number of new neurons functionally active within the OB, which associates with an improvement in olfactory performance strictly dependent on adult SVZ neurogenesis, i.e., the odor detection threshold and short-term olfactory memory. These data suggest that in the adult SVZ of p21 KO mice, NSCs retain a high neurogenic potential, triggered by physical activity, with long-term consequences in olfactory-related behavior.

Keywords Adult neurogenesis · Subventricular zone · Physical activity · Cell cycle · p21 · Olfactory behavior

Introduction

Neurogenesis, the generation of new neurons originating from neural stem cells, occurs throughout life but is gradually lost with age or neurodegenerative diseases [1–3]. A number of studies have focused on neurogenesis during different adult stages, demonstrating the impact of several factors, including physical activity, olfactory experience, and stressful inputs, as important modulators for shaping this process [4–9]. However, several issues remain to be elucidated concerning the neurobiological mechanisms sustaining neurogenesis in the adult brain.

Here, we analyze the p21 knockout mouse to investigate the impact of physical activity on a mouse model characterized by defective adult subventricular neurogenesis. In our study, we included behavioral analysis in the p21 knockout (KO) mice model in order to elucidate the effect of voluntary running on subventricular zone (SVZ) neurogenesis-dependent olfactory functions.

In the SVZ of the adult brain, new neurons were derived from a subpopulation of slowly dividing astrocyte-like neural stem cells (NSCs) named type B cells [10–12], which give rise to type C cells, a class of transit-amplifying progenitors (TAPs) that rapidly divide into neuroblasts named type A cells. Type A cells exit the cell cycle and migrate along the rostral migratory stream (RMS) to the olfactory bulb (OB) [13, 14], where they move toward the granule and glomerular

Electronic supplementary material The online version of this article (https://doi.org/10.1007/s12035-019-1590-6) contains supplementary material, which is available to authorized users.

✉ Stefano Farioli Vecchioli
Stefano.FarioliVecchioli@cnr.it

[1] Institute of Cell Biology and Neurobiology, National Research Council, Via E. Ramarini, 32, 00015 Monterotondo (RM), Italy

[2] European Brain Research Institute (EBRI), Viale Regine Elena, 00161 Rome, Italy

[3] Laboratory of Neuroimmunology, Fondazione Santa Lucia, Via del Fosso di Fiorano 64, 00143 Rome, Italy

cell layers and finally mature into GABAergic inhibitory interneurons [15–17]. SVZ neurogenesis is positively regulated by olfactory experience: odor exposure improves the survival and functional integration of new neurons which, in turn, leads to enhanced olfactory memory, thereby indicating a prominent role for SVZ neurogenesis in olfactory behavior [18, 19].

The majority of NSCs in the adult SVZ persist in a quiescent state and are rarely recruited into the cell cycle. Quiescent NSCs function as a reserve pool for preserving the NSC longevity, retaining genomic integrity throughout life and producing new neurons to counteract neurodegenerative processes following brain damage [20]. However, over time, quiescent NSCs lose their ability to enter the cell cycle, with consequent decrease of the cell pool size and exhaustion of neurogenesis in the aging brain [21, 22]. Hence, understanding the processes involved in maintenance over time of NSC pool can provide relevant information to the studies of adult neurogenesis.

Among the main regulators of adult NSC transition between quiescence and differentiation, a central role is exerted by the Cip/Kip family of CKIs, which comprises $p21^{Waf1/Cip1}$ (hereafter referred to as p21), $p27^{Kip1}$, and $p57^{Kip2}$ [23, 24]. These proteins negatively regulate cell cycle progression by directly binding and inhibiting cyclin-CDK complexes. In particular, p21 is a key mediator of the p53-induced G1 checkpoint via the binding to and inactivation of G1-associated cyclin A– and cyclin E–containing cyclin/CDK complexes [25–27]. In neurogenic niches, p21 plays a dual role, maintaining NSC quiescence and restraining progenitor proliferation [28–30]. In p21 KO mice, a rapid activation of quiescent NSCs in the post-natal stage has been reported; this reduces NSC self-renewal capacity and causes replicative stress in the hyper-proliferating progenitors, thereby demonstrating that exhaustion of NSCs impairs neurogenesis [31–33].

While the lack of p21 is associated with gradual reduction of NSCs and SVZ neurogenesis, it is unclear whether adult p21-null NCSs can keep their pro-neurogenic potential. In order to deepen this issue, we decided to focus on the potential of running to serve as modulator to disclose the putative enhanced neurogenic properties owned by p21-lacking NSCs.

Physical exercise generates a considerable rise in cell proliferation and in newborn neuron survival, maturation, and functional integration in the adult rodent DG [5, 34–36]. In rodent models, voluntary running improves hippocampus-dependent learning and memory, mitigates the severity of deficits caused by behavioral disorders and traumatic brain injury (TBI), and contrasts the onset as well as the pathological progression of neurodegenerative diseases [37–39]. Even if it has been extensively demonstrated that the SVZ niche is refractory to the pro-neurogenic stimulus provided by physical exercise [40–44], our recent study has shown that in mice lacking the cell cycle inhibitor BTG1, 12 days of voluntary physical activity are able to activate NSCs and to improve neurogenesis not only in DG but also in SVZ [44, 45]. These data suggest that cell cycle modulation might have a strong impact in running-associated activation of NSCs.

In this paper, our results demonstrate that the combination of running and of p21 knockdown massively increases neurogenesis in the SVZ of p21 KO mice. In particular, we found that running induces the activation and expansion of the p21-devoid NSC pool, coupled with cell cycle modification and a faster migration of post-mitotic neuroblasts. These events contribute to maximize the self-renewal potential of NSCs, the functionality of the SVZ-OB axis, and the activation of newborn neurons as indicated by c-fos expression analysis. Remarkably, such modifications are accompanied by the enhancement of the olfactory behavior in p21 knockout running mice. Finally, neurosphere assay performed in p21/Nestin GFP^+ mice indicates that the increase in the self-renewal and in proliferative activity triggered by running is a cell-intrinsic process.

Material and Methods

Animals

Male wild-type and p21-null mice [46] of the same genetic background (129Sv/c57BL6; 50:50; https://www.jax.org/strain/003263) were housed under a continuous 12-h light/12-h dark cycle at a constant temperature of 21°, with complete availability of water and food. Genomic extraction of DNA followed by genotyping was carried out from tail samples and performed as previously described [47]. Male Nestin-green fluorescent protein mice (c57BL6 background; kindly provided by Dr. G. Enikolopov) express GFP driven by the Nestin promoter [48]. Nestin-GFP mice were crossed with p21 WT and knockout mice to obtain p21 WT and KO/Nestin GFP^+ mice which were interbred at least four times before further analysis, in such way generating the different genotypes under study. Genotyping of Nestin-GFP pups was performed using a "GFP flashlight" (Nightsea) that made the GFP^+ pups glow.

At 2 and 12 months of age, animals were subjected to voluntary physical exercise by positioning them in pairs in standard cages with free access to a running wheel where they were left for 5, 12, or 21 days. The distance covered was recorded daily on an automatic counter and after the designated exercise period, mice were sacrificed or returned to standard cages to be sacrificed at different times from the end of the run. The average daily running distance calculation did not reveal any significant difference between p21 WT and KO running at 2 and 12 months of age (data not shown). Animals were treated following the Italian Ministry of Health and directive 2010/63/EU guidelines.

Immunohistochemistry

Following transcardiac perfusion with 4% paraformaldehyde (PFA) in phosphate-buffered saline (PBS), the brains were collected and kept overnight at − 4 °C in PFA. They were subsequently equilibrated in sucrose diluted at 30% and finally cryopreserved at − 80 °C. Slicing was carried out by embedding the brain in *Tissue-Tek* OCT (Sakura, Torrence, CA, USA) and then cut using a cryostat at − 25 °C throughout the whole rostro-caudal extent. The coronal sections were processed in a one-in-six series protocol at a 40-μm thickness. Sections were then stained for multiple labelling using different fluorescence techniques. Sections were initially washed with glycine 0.1 M for 10 min followed by permeabilization using 0.3% Triton X-100 in PBS for another 10 min. The sections were then incubated for 30 min in a blocking solution containing 3% normal donkey serum (NDS) in 0.3% Triton X-100 in PBS to saturate the specific sites, followed by incubation with the same blocking solution containing primary antibodies for 16–18 h at 4 °C. The primary antibodies used were mouse monoclonal antibodies raised against Nestin (Millipore Cat# MAB353; 1:100), NeuN (Millipore Cat# MAB377; 1:300), GFAP (Sigma-Aldrich Cat# G3893; 1:400), and pHH3 (Cell Signaling Technology Cat# 9706; 1:100); goat polyclonal antibodies were used against DCX (Santa Cruz Biotechnology; Cat# Sc-8066; 1:300) and SOX2 (Santa Cruz Biotechnology Cat# sc-8066; 1:300); a rabbit monoclonal antibody was used against Ki67 (Lab Vision Cat# RM-9106-S; 1:150) and a rabbit polyclonal antibody against c-fos (Millipore Cat# PC38; 1:500) and gamma H2A.X (Abcam Cat# ab11174; 1:100). To observe primary antibody binding, donkey secondary antibodies conjugated to Cy2 (Jackson Immunoresearch, West Grove, USA; 1:200 in PBS), Cy3 (Jackson ImmunoResearch, West Grove, PA, USA; 1:300 in PBS), or Alexa-647 (Invitrogen, San Diego, CA, USA; 1:300 in PBS) were used. Nuclei were observed incubating sections with Hoechst (1:500). The estimation of cell numbers throughout the entire rostro-caudal extent of the SVZ and in OB was carried out with stereological analysis, by counting cells expressing the indicated markers, visualized with Leica Sp-5 confocal microscopy, in one-in-ten series of 40 μm free-floating serial coronal section (240 μm apart). Cell number for each SVZ and OB section was divided by the corresponding area of the individual section [44, 49], to calculate the average number of cells per 100 μm^3 of SVZ and OB volume. Region of interest was calculated by tracing the outline of the desired structure, identified by the presence of nuclei stained with Hoechst 33258, on a digital picture captured using ImageJ system, which was also used to count the labeled cells. The running animals were placed in pairs in cages provided with wheels. At least 4 male mice per condition were analyzed (sedentary or running). The ImageJ was used to count labeled cells.

BrdU and Thymidine Analog Detection

In order to calculate the cell cycle exit, mice at P60 were treated with a single bromodeoxyuridine (BrdU, 95 mg/kg i.p.) pulse and sacrificed 48 h after. To label SVZ-newborn neurons migrating through the rostral migratory stream (RMS) toward the OB, animals were treated with five daily injections of BrdU followed by perfusion 7 days from the last injection. Finally, mature neurons within the olfactory bulb were detected after treating the mice with five daily injections of BrdU. Twenty-eight days after the last BrdU injection, an olfactory stimulation protocol was applied and animals were then perfused. Detection of BrdU-positive cells consisted in denaturing DNA with 2N HCl for 45 min at 37 °C to facilitate antibody access. The sections were then incubated with 0.1 M sodium borate buffer at pH 8.5 for 2–10-min intervals followed by overnight incubation at 4 °C with a rat anti-BrdU primary antibody (Abcam Cat# ab6326; 1:300) diluted in TBS containing 0.1% Triton, 0.1% Tween, and 3% normal donkey serum (blocking solution). Immunohistochemistry performed against IdU and CldU consisted in a 10-min incubation with 2N HCl and the normal donkey serum was used at 5% in order to provide more stringent conditions to avoid cross-reactivity between antibodies. Following incubation with the primary antibodies, the sections were washed five times with TBS for 5 min each time. Detection of the halogenated thymidine analogs was performed using mouse anti-BrdU (BD Biosciences; B44 1:500) for IdU and rat anti-BrdU (Abcam Cat# ab6326; 1:300) for CldU.

Cell Cycle Analysis

To measure the precise length of the S-phase (Ts) and the overall length of the cell cycle (Tc), the thymidine analogs IdU (5-iodo-2-deoxyuridine) and CldU (5-chlorodeoxyuridine) were used following a protocol developed by Brandt [50]. To specifically calculate the Ts, mice at P60 received a single i.p. injection of 57.5 mg/kg of IdU dissolved in 0.2N NaOH and 0.9% NaCl solution; 3 h later, the same animals received 42.5 mg/kg dissolved in 0.9% sterile NaCl CldU injection followed by sacrifice 45 min later. The 3-h time interval between injections allowed the generation of three different cell populations: $CldU^+/IdU^-$ cells, which entered the Ts phase during the 3-h gap, $IdU^+/CldU^-$ cells that exited the S-phase in between the two injections, and the double-positive $IdU^+/CldU^+$ cells that were found in the S-phase during both injections. According to the equation created by the same authors, the ratio between the $IdU^+/CldU^-$ cell population and the total IdU cells is equals the ratio between the 3-h intra-injection interval and the S-phase.

Likewise, to calculate the overall length of the cell cycle (Tc), IdU and CldU injections were administered 16 h apart,

and the animals were sacrificed 45 min afterwards. We subsequently estimated the length of the G2/M phase by calculating the percentage of labeled mitoses. To this aim, the animals were subjected to a single BrdU pulse (i.p. 95 mg/kg in saline) followed by perfusion 1.5, 3, and 5 h later. Immunohistochemistry against BrdU and PH3 (phosphohistone 3 which marks mitotic cells) was performed; the time elapsed between the injection and the time point at which all cells resulted $PH3^+$ corresponded to the duration of G2/M. Finally, the length of the G1 phase was calculated by the following formula: $T_{G1} = Tc–(Ts + T_{G2/M})$, where T_{G1} and $T_{G2/M}$ represent the length of G1 and G2/M phases, respectively.

Olfactory Stimulation

To evaluate the functional activation of new neurons within the OB following physical exercise, mice at P60 were subjected to an olfactory stimulation test, followed by an immunofluorescent analysis of the expression of the immediate early gene (IEG), c-fos. Mice were positioned in cages identical to the ones utilized to house them but lacking the wood chip bedding; filter paper soaked in 3% octanal diluted in mineral oil was then positioned in a chosen corner of the cage. During the following 35 min, the animals were exposed to the odorant for 5 min followed by a 5-min interval (three sessions in total); after the last session, they were left in the test cage for additional 60 min before being sacrificed. New neurons activated by olfactory stimulation were quantified through immunohistochemistry by concurrent expression of $BrdU^+/NeuN^+$ and the IEG c-fos.

Open Field Test

Spontaneous exploratory locomotor activity and thigmotaxis in the open field were used as a general measure of motor function and anxiety-related behaviors, respectively [51]. At the beginning of each trial, mice at P60 were placed in the center of a circular white open field arena having a diameter of 100 cm, for 20 min. The arena was cleaned with 70% ethanol to avoid cue smell between each trial. The room was brightly lit, which in combination with the exposure to novel environment and open space induce anxiety in rodents. Thus, anxiogenesis was measured by time spent in center vs. time spent in the periphery of the open field arena. Locomotor activity was measured by distance traveled and average speed over the 20 min of exploration, where a large distance traveled and increased velocity are indicative of hyperactivity [52]. Both thigmotaxis and locomotor activity were measured and analyzed using a specialized software with tracking system (Ethovision XT 8.5, Noldus Information Technology, USA).

Olfactory Detection Threshold

The test was performed as previously described [53, 54], with minor modifications. Starting 4 days before the test, mice at P60 were caged individually and cages were never changed or cleaned up, so that they would get used to background odors. Two separate cotton swabs were presented simultaneously at opposite corners of the cage: the first was soaked with mineral oil; the second was soaked with octyl aldehyde or butyl-butyrate at increasing concentrations (10^{-7}, 10^{-5}, 10^{-4}, and 10^{-3}%) during the different sessions. In each of four daily sessions, the animals were exposed to the cotton swabs for 3 min; each day, the swabs were located in different positions within the cage to avoid spatial learning. Each session was video-recorded in order to measure the amount of time the animals spent sniffing at the cotton swabs, which was defined as nasal contact with the tip of the swab. An odor detection index was calculated as the ratio between the time spent sniffing at the odorant and the total time spent sniffing at both swabs (odorant plus mineral oil). Values higher than 50% indicated a preference for the odorant over the mineral oil.

Olfactory Short-Term Memory

Using the same procedure as described above, mice at P60 were exposed to a single cotton swab; this was laced with the same odor at the same concentration (10^{-3}%) during two different 5-min sessions separated by 30, 240, 300, and 360 min in the four consecutive testing days, respectively, with different odorants every day. The designated odors were acetophenone, limonene, octanal, and carvone (+), and the cotton swab was inserted in the same position for the sessions performed on the same day but was changed every consecutive day. An olfactory memory of the first presentation to the odorant is manifested in a decline in the time spent investigating the swab during the second exposure.

GFP^+ Neural Stem Cell Cultures

Mice at P60 were euthanized by cervical dislocation and the brains were removed. SVZs were dissected out and cells were isolated by enzymatic digestion (1.33 mg/mL trypsin, 0.7 mg/mL hyaluronidase, and 0.2 mg/mL kynureinic acid) for 30 min at 37 °C and then by mechanical dissociation with a small-bore Pasteur pipette. The cell resuspension was then passed through a 30-mm cell strainer (BD Bioscience), resuspended in PBS, and GFP^+ cells were separated by fluorescence-activated cell sorting (FACS) on a MoFlo high-speed cell sorter (Beckman Coulter). Isolated GFP^+ NSCs were cultured in DMEM/F12 medium supplemented with

B27, EGF, and bFGF (20 and 10 ng/mL, respectively). To perform the neurosphere assay, GFP^+ cells were cultured under clonal conditions, in which neurospheres (NSFs) are generated from single cells and serve as an index of the number of in vivo NSCs. GFP^+ cells were plated at 10 cells/μL in 24-well uncoated plates in growth medium. The total number of GFP^+ neurospheres was analyzed every 7th day of culture. The size of GFP^+ NSFs was expressed as a volume calculated from the measurement of their diameter in picture taken by fluorescent microscopy (Leica DM IRB). Following the assay, the NSFs were mechanically dissociated into single cells that were plated under clonal conditions. To evaluate expansion capacity, primary GFP^+ neurospheres were dissociated into single cells and plated at the same clonal density. Then, secondary neurospheres were dissociated, and the number of cells was determined and expressed as average expansion from the initial starting population (number of cells from secondary neurospheres at 7 DIV/number of seeded cells).

Experimental Design and Statistical Analysis

Parameters linked to SVZ adult neurogenesis were preliminarily analyzed by two-way ANOVA, with genotype (WT, KO) and treatment (no run, run 5d, run 21d, run 21d) as independent variables, followed by Fisher's protected least significant difference (PLSD) post hoc test. In agreement with previous studies, running was found not to exert any significant effect on SVZ adult neurogenesis in WT mice, regardless of the running regimen. For this reason, with the aim of reducing as much as possible the number of experimental animals to be sacrificed, only WT sedentary mice were included in subsequent experiments, and the related data were analyzed by one-way ANOVA, followed by Fisher's PLSD test, assuming WT no run, KO no run, KO run 5d, KO run 12d, and KO run 21d as independent groups. For the sake of maximum clarity, the data are analyzed, plotted, and discussed this way (i.e., with the exclusion of trained WT mice) throughout the manuscript. Data from the odor detection test were analyzed by two-way ANOVA, with group (WT no run, KO no run, KO run 5d, KO run 12d) and odorant concentration (10^{-7}%, 10^{-5}%, 10^{-4}%, 10^{-3}%) as independent variables, followed by Fisher's PLSD post hoc test. A single sample t test was performed to confirm that the odor detection index was significantly higher than 50%. Finally, in both the open field test (OFT) and olfactory short-term memory (STM) tests, Student's t test was performed to compare the animal locomotor activity (in the OFT) and the duration of sniffing (in the STM). Differences were considered statistically significant at $p < 0.05$. All data are expressed as mean values ± SEM.

Results

Five and 12 Days of Physical Exercise Results in a Consistent Induction of SVZ Neurogenesis in 2-Month-Old p21 KO Mice

To study the effect of physical activity on the SVZ neurogenesis of p21 wild-type (p21 WT) and knockout (p21 KO) mice, the animals were put in cages provided with free-access running wheels and subjected to three different paradigms of running: 5 days (p21 KO run 5d), representing the acute run protocol, 12 days (p21 KO run 12d) that has been previously demonstrated to cause the peak of running-dependent pro-neurogenic effects [44, 45], and 21 days (p21 KO run 21d), characterizing long-term voluntary exercise. A two-way ANOVA, with «genotype» and «training» as independent variables, was preliminarily performed on a number of parameters linked to SVZ neurogenesis, which detected, with no exception, a significant «genotype × training» interaction ($F > 4.05$, $p < 0.01$). Post hoc comparisons indicated that running did not exert any significant effect on SVZ neurogenesis in WT mice, regardless of the running regime they were submitted to ($p > 0.59$; Table 1). This result came in full agreement with previous literature showing that adult SVZ is normally refractory to physical exercise as a neurogenic stimulus [40, 44]. For this reason, p21 WT running animals were not included in subsequent experiments, and p21 WT sedentary mice were maintained as the only control group with which both p21 KO sedentary mice and p21 KO run mice would be compared. Also, in agreement with previous studies comes the observation that, at 2 months of age, sedentary p21 WT and KO mice did not show significant differences ($p > 0.28$) in the expression of markers specific to NSCs and neural progenitors residing in the SVZ (Figs. 1 and 2). These results confirm that adult SVZ neurogenesis begins to decline after such an age in p21 KO mice [31, 55].

We first investigated how the different running patterns might influence the recruitment of the type B NSCs in the cell cycle and their expansion. The quantification of the specific type B markers SOX2/GFAP and the proliferative marker Ki67 revealed that 5 and 12 days of running induced in the p21 KO mice a significant increment in the recruitment from quiescence of type B cells (expressed as the ratio between $Ki67^+/SOX2^+/GFAP^+$ cells to the total $SOX2^+/GFAP^+$ cells), when compared with the sedentary p21 WT and KO mice ($F_{(4, 56)} = 6.65$, $p < 0.001$, one-way ANOVA followed by Fisher's PLSD post hoc test; Fig. 1a–e, f). This event induces a significant increase in the type B pool size, assessed by counting of $SOX2^+/GFAP^+$ cells density (Fig. 1a–e, h) and of the overall proliferating cells ($Ki67^+$; Fig. 1a–e, i) in the p21 KO run 5d and 12d in respect to the other experimental conditions under investigation ($SOX2^+/GFAP^+$: $F_{(4, 55)} = 7.57$, $p < 0.001$, one-way ANOVA followed by Fisher's PLSD post hoc test; Ki67:

Table 1 Effect of running on SVZ neurogenesis in the 2-month-old p21 wild-type mice

	Ki67	GFAP	Ki67 GFAP	% Recruitment	Nestin	Ki67 Nestin	DCX	Ki67 DCX
WT	9573 ± 501	4069 ± 311	460 ± 78	13,88 ± 2,23	7964 ± 725	4344 ± 205	5552 ± 367	5324 ± 477
WT run 5d	8983 ± 620	3793 ± 281	416 ± 59	13,46 ± 1,68	7904 ± 1067	4157 ± 485	5986 ± 346	5592 ± 347
WT run 12d	8975 ± 523	3749 ± 321	480 ± 90	13,38 ± 2,20	8440 ± 537	4068 ± 335	5296 ± 3,46	4929 ± 136
WT run 21d	10,037 ± 628	3821 ± 331	452 ± 64	14,57 ± 1,59	7806 ± 401	4021 ± 309	5232 ± 565	5475 ± 420

Values are expressed as cell density (number of positive cells/ 100 μm^3 SVZ) ± SEM

% Recruitment is expressed as ratio between total number of Ki67$^+$/GFAP$^+$ cells on total number GFAP$^+$ cells

The table shows the main parameters related to adult neurogenesis, measured in the SVZ of the sedentary p21 WT mice and of the p21 WT mice submitted to the three different running conditions (5, 12, and 21 days). Statistical analysis through ANOVA does not show any significant difference in the comparisons between the p21 WT mouse parameters and those measured in p21 WT mice after different running conditions

$F_{(4,\ 132)} = 15.66$, $p < 0.0001$, one-way ANOVA followed by Fisher's PLSD post hoc test). In agreement with previous findings demonstrating that p21 negatively regulates SOX2 expression [32], we found a significant increase of SOX2$^+$ cells in the p21 KO SVZ in comparison with WT mice ($F_{(4,\ 56)} = 6.53$, $p = 0.0004$, one-way ANOVA followed by Fisher's PLSD post hoc test; Fig. 1a–i, j). Moreover, we observed that 5 and 12 days of running maintains the increased of SOX2$^+$ cell population, while after 21 days, a drastic decrease of these cells, which returned to the WT level, occurred ($F_{(4,\ 56)} = 6.15$, $p < 0.001$, one-way ANOVA followed by Fisher's PLSD post hoc test; Fig. 1j). To this regard, we observed that 21 days of running did not exert any pro-neurogenic effect in the SVZ of p21 KO mice (Fig. 1e–j). The above results suggested that p21-lacking NSCs have a substantial reservoir for activation and expansion in the presence of a pro-neurogenic stimulus, such as physical activity.

To further analyze this intrinsic pro-neurogenic potentiality of p21-null NSCs after running, we studied the following differentiative stages of adult SVZ neurogenesis of p21 KO mice subjected to the three running paradigms. Our results showed that in p21 KO mice, 5 and 12 days of running triggered a consistent increase of proliferation of Nestin$^+$ cells, which comprise the type B and type C SVZ subpopulation (Ki67$^+$/Nestin$^+$ cells; Fig. 2a–e, f), and of the type A neuroblasts (Ki67$^+$/DCX$^+$ cells; Fig. 2a–e, g), largely exceeding physiological values (Ki67$^+$/Nestin$^+$: $F_{(4,\ 73)} = 29.2$, $p < 0.001$, one-way ANOVA followed by Fisher's PLSD post hoc test; Ki67$^+$/DCX$^+$: $F_{(4,\ 69)} = 14.0$, $p < 0.001$, one-way ANOVA followed by Fisher's PLSD post hoc test). Consequently, we observed a significant expansion of Nestin$^+$ cells (Fig. 2h) and type A (DCX$^+$ cells; Fig. 2i) subpopulations residing in the SVZ of 5 and 12 days of running p21 KO mice, when compared with sedentary p21 WT and KO groups (Nestin$^+$: $F_{(4,\ 74)} = 10.3$, $p < 0.001$, one-way ANOVA followed by Fisher's PLSD post hoc test; DCX$^+$: $F_{(4,\ 67)} = 15.8$, $p < 0.001$, one-way ANOVA followed by Fisher's PLSD post hoc test). Also in this case, we found that no marked changes in the type C and type B subpopulations between the p21 WT and KO mice occurred (Fig. 2f–i) and that the 21 days running session did not provide any pro-neurogenic effects in the SVZ of p21 KO mice with respect to the sedentary counterpart (Fig. 2f–i).

All together, these data clearly indicated that in the absence of the cell cycle inhibition exerted by p21, an external pro-neurogenic stimulus such as running was sufficient to highly enhance the SVZ neurogenesis above the physiological parameter, as a result of an increased recruitment of quiescent NSCs and their ensuing proliferative capacities, leading to a large boost of the immature neuroblast pool. Moreover, our results suggested that a prolonged period of physical activity (21 days) did not exert any beneficial effect on p21 KO SVZ neurogenesis, likely due to an excessive proliferative activity that might induce the appearance of replicative stress in the

Fig. 1 Five and 12 days of running triggers an increase of NSC recruitment and expansion in p21 KO mice. Increased recruitment from quiescence and expansion of NSCs in p21 KO mice after 5 and 12 days of running. (**a**–**e**) Representative fluorescence confocal images of SVZ coronal sections showing the increased recruitment and expansion of Ki67$^+$/SOX2$^+$/GFAP$^+$ dividing type B neural stem cells (in red, blue, and green, respectively) in the SVZ of p21 KO run 5d and 12d mice (scale bar, 100 μm). **f** The percentage of type B cells recruited in cell cycle (ratio between Ki67$^+$/SOX2$^+$/GFAP$^+$ and total SOX2$^+$/GFAP$^+$ cells) is significantly enhanced in p21 KO run 5d and 12d with respect to WT animals (p21 WT vs. p21 KO run 5d, $p = 0.001$ and vs p21 KO run 12d, $p < 0.05$). **g**–**i** Quantification of the cell density (total number of labeled cells/SVZ area) for the different markers, demonstrating that running triggers subventricular neurogenesis in the SVZ of p21 KO run 5d and 12d mice. **g** Histogram showing a significant increment in the p21 KO run 5d and 12d mice in respect to the p21 WT mice of the cycling type B cells (Ki67$^+$/SOX2$^+$/GFAP$^+$: p21 KO run 12d vs. p21 WT, $p < 0.05$ and vs. p21 KO, $p < 0.01$). **h** And of the type B pool size (SOX2$^+$/GFAP$^+$: p21 KO run 12d vs. p21 WT, $p < 0.001$ and vs. p21 KO, $p < 0.05$). **i** These events lead to an overall increased proliferation (Ki67$^+$ cells) in the SVZ of p21 KO run 5d and 12d mice in respect to the p21 WT mice (p21 KO run 12d vs. p21 WT, $p < 0.01$ and vs. p21 KO, $p < 0.01$). **j** Graph illustrating the enhancement of SOX2 expression in the p21 KO and p21 KO run 5d and 12d mice in respect to the p21 WT mice. Cell density (cell number/volume SVZ) is mean ± SEM of the analysis of at least four animals per conditions. Statistical significance: *$p < 0.05$, **$p < 0.01$, ***$p < 0.001$. ANOVA analysis

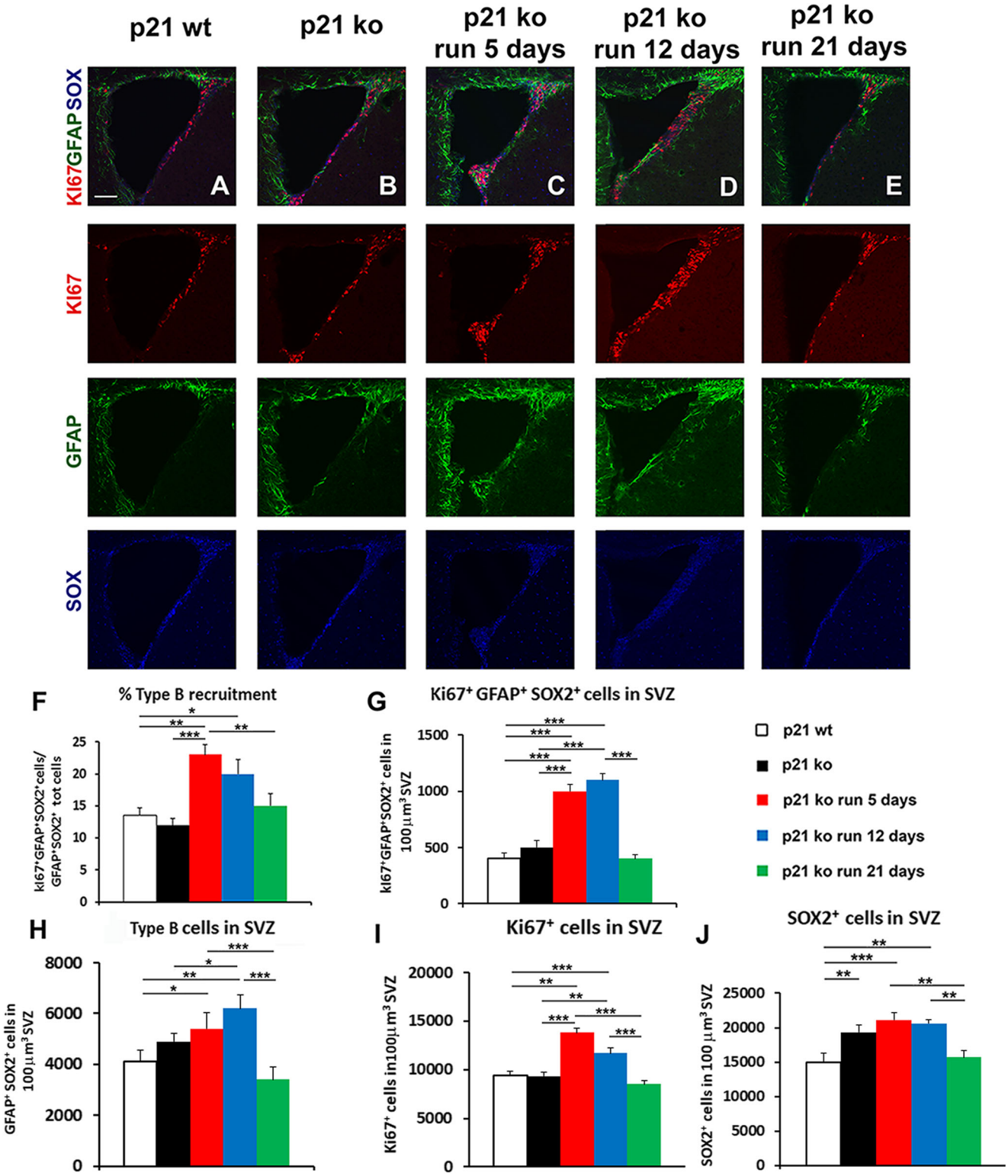

hyper-proliferating progenitors. In order to verify our hypothesis, we performed an immunostaining for phosphorylated H2AX (γH2AX), which represents a specific marker of replicative stress, and we observed a significant induction of γH2AX in the SVZ of p21 KO run 21d mice in comparison with the other experimental conditions ($F_{(4,\ 31)} = 2.87$, $p < 0.05$, one-way ANOVA followed by Fisher's PLSD post hoc test; Supp. Fig. 1).

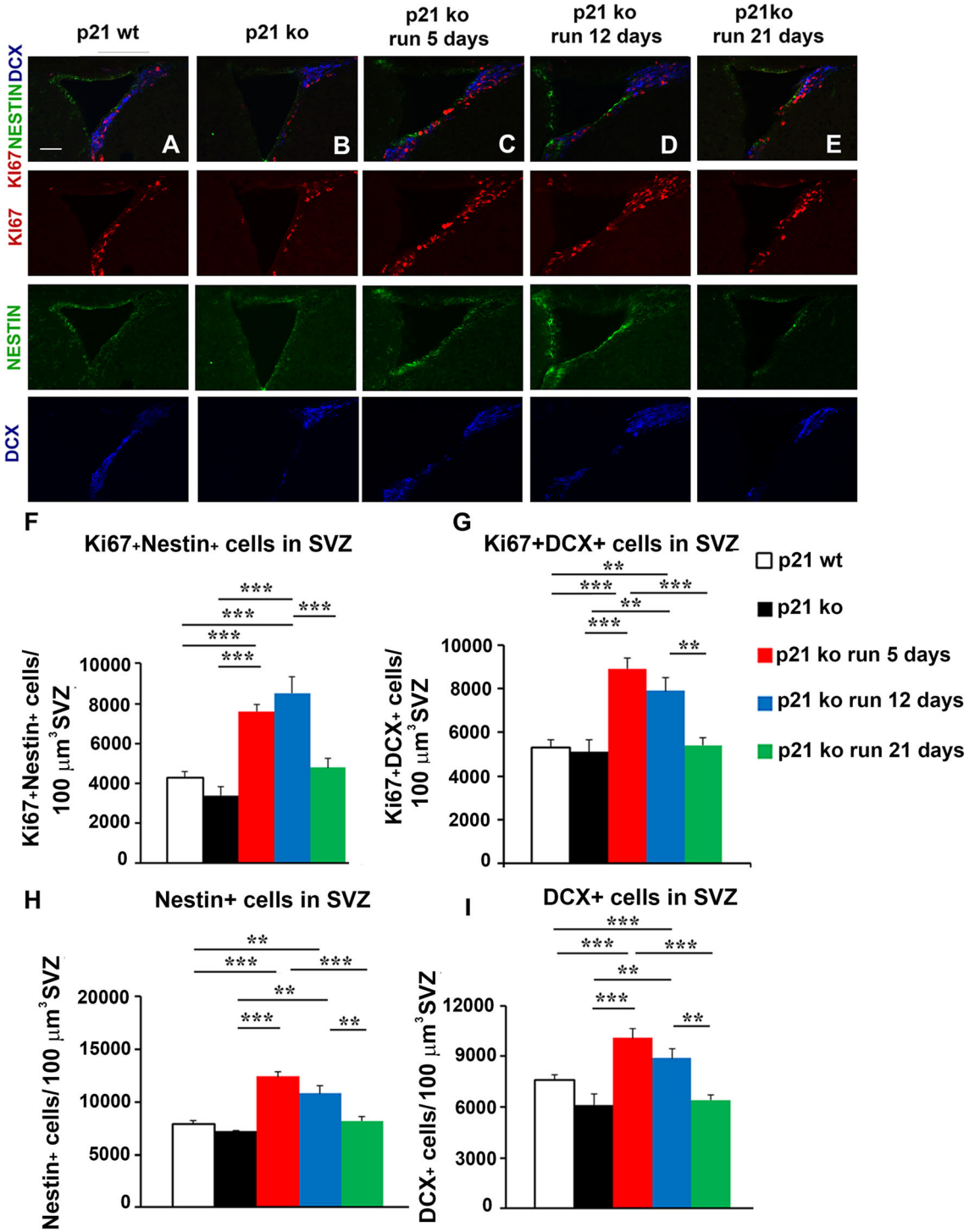

Fig. 2 Five and 12 days of running enhance type C and type A subpopulation in p21 KO mice. Enhanced adult SVZ neurogenesis in p21 KO mice after 5 and 12 days of running. **a**–**e** Representative confocal images of SVZ coronal sections illustrating the large increase in the p21 KO run 5d and 12d mice of Nestin$^+$ (identifying type B and type C cells) and type A cell number, recognized as triple-labeled Ki67$^+$/Nestin$^+$/DCX$^+$ cells, in red, green, and blue, respectively (scale bar, 100 μm). **f**–**g** Histogram showing the enhanced number of proliferating type B/C (Ki67$^+$/Nestin$^+$) and type A cells (Ki67$^+$/DCX$^+$) in the 5- and 12-days running p21 KO mice largely exceeding the values measured in the other conditions (Ki67$^+$/nestin: p21 KO run 5d vs. p21 WT, $p < 0.001$, p21 KO run 12d vs. p21 WT, $p < 0.001$; Ki67$^+$/DCX$^+$: p21 KO run 5d vs. p21 WT, $p < 0.001$, p21 KO run 12d vs. p21 WT, $p < 0.001$). **h**–**i** The overall number type B/C cells and type A cells, identified as Nestin$^+$ and DCX$^+$ cells, respectively, was significantly increased when compared with the control experimental conditions (Nestin$^+$: p21 WT vs. p21 KO run 5d, $p < 0.001$, vs. p21 KO run 12d, $p < 0.01$; DCX$^+$: p21 WT vs. p21 KO run 5d and vs. p21 KO run 12d, $p < 0.001$). Cell density (cell number/volume SVZ) is mean ± SEM from the analysis of at least four animals *per* condition. Statistical significance: $*p < 0.05$, $**p < 0.01$, $***p < 0.001$. ANOVA analysis

Twelve Days of Running Shortens the G1 Phase and Cell Cycle Length in the Proliferating Cells in the SVZ of p21 KO Mice

To directly determine if the enhanced proliferation rate observed in the p21 KO run 5d and in the KO run 12d mice was dependent on modification of the cell cycle, we performed two different cell cycle analyses: the cell cycle length calculation [44, 45, 50] and the cell cycle exit measurement. The first methodological approach was characterized by two different time-points between injections of the BrdU analog, Idu, and CldU, in order to accurately measure the length of the S-phase (Ts, 3-h time-point; Fig. 3a, b, d) and the total cell cycle length (Tc, 16-h time-point; Fig. 3e, f, h). The analysis showed that p21 deletion did not affect the Ts in sedentary mice (Ts p21 WT = 9.48 ± 0.83 h; Ts p21 KO = 9.27 ± 0.55 h; Fig. 3c, i), and also that the three different running protocols did not exert any significant alterations in the S-phase of the p21 KO mice ($F_{(4,\ 52)} = 0.76$, $p = 0.55$; Fig. 3c, i). The calculation of the whole cell cycle length (Tc; Fig. 3e, f, i) displayed a significant shortening of the cell cycle length in the p21 KO run 12d (Tc = 16.8 ± 0.08) mice in respect to the p21 WT and p21 KO mice (Tc p21 WT = 17.6 ± 0.2; Tc p21 KO = 17.6 ± 0.11, $F_{(4,\ 39)} = 11.7$, $p < 0.001$, one-way ANOVA followed by Fisher's PLSD post hoc test; Fig. 3g, i), while 5 days of running was not able to induce a faster progression of the cell cycle in the p21 KO mice (Tc p21 run 5d = 17.4 ± 0.3; Fig. 3g, i). Finally, we observed in the p21 KO run 21d a significant increment in the cell cycle duration (Tc = 19 ± 0.34) when compared with the other experimental conditions ($F_{(4,\ 39)} = 11.7$, $p < 0.001$, one-way ANOVA followed by Fisher's PLSD post hoc test; Fig. 3g, i), further confirming that a prolonged period of running might induce a consistent lengthening in the cell cycle progression of the SVZ p21-lacking progenitors. To better analyze the kinetic of the different cell cycle phases, we also measured the length of G2/M, by using the percentage of labeled mitotic index (see M&M for more specific information), and we found that the G2+M phase length was about 5 h for all the experimental groups (Fig. 3i). Consequently, the calculation of the G1 phase was carried out by subtracting the S-phase and G2/M phases from the Tc [56], and it clearly showed that in the SVZ of p21 KO mice, 12 days of running was able to significantly shorten the G1 phase in comparison with the other experimental groups ($F_{(4,\ 37)} = 2.88$, $p < 0.05$, one-way ANOVA followed by Fisher's PLSD post hoc test, Fig. 3i). Afterwards, we decided to assess the possibility that the increased proliferation observed in the 5 and 12 days running p21 KO mice was strictly dependent on a longer permanence of running-activated SVZ progenitors in the cell cycle. To this goal, we determined the cell cycle exit rate of neural progenitors residing in the SVZ by injecting animals with a single BrdU pulse and performing immunostaining for BrdU and Ki67 48 h later (Supp. Fig. 2 A). The fraction of cells exiting the cell cycle after this time interval was calculated by dividing the number of $BrdU^+/Ki67^-$ cells by the total number of $BrdU^+$ cells. From the results obtained, we observed that in the p21 KO run 5d and 12d mice, the percentage of newborn neurons that have exited the cell cycle after 48 h dramatically decreased when compared with the values seen in the p21 WT and KO mice. Moreover, the fraction of cells exiting the cell cycle in the p21 KO run 21d running animals drastically increased in respect to p21 KO run 12d ($F_{(4,\ 33)} = 7.692$, $p < 0.001$, one-way ANOVA followed by Fisher's PLSD post hoc test; Supp. Fig. 2 B), reaching the percentage observed in sedentary WT mice.

Overall, the cell cycle analysis suggests that in the p21 KO mice, the 12-days running paradigm was able to shorten the cell cycle length and to decrease the proportion of cells exiting the cycle, thereby allowing them both a longer permanence inside it and the possibility to perform a greater number of cell divisions, ultimately leading to the overall increase in proliferation. Moreover, the cell cycle lengthening and the increased percentage of neuroblasts exiting from the cell cycle observed in the 21-days running paradigm demonstrates that this condition induces a reduction in the number of achievable cycles and consequently a significant decrease in progenitor proliferation, confirming the absence of pro-neurogenic effects exerted by a sustained period of running in the p21 KO mice. However, we did not observe any causal correlation between the increase in proliferation and changes in G1 and/or whole cell cycle length after 5 days of running in the p21 KO mouse. In this regard, we can only hypothesize that even a slight reduction in the cell cycle length detected after a short-term running session was sufficient to trigger a significant increase in proliferation in the absence of p21.

Running Induces a Faster Migration of Post-Mitotic Neuroblasts in the p21 KO Mice

Adult SVZ neuroblasts, once out of the cell cycle, migrate through the rostral migratory stream (RMS) in order to reach their final destination, the olfactory bulb (OB), where they mature into granule cells (GCs) and periglomerular cells (PGCs). These cells play a pivotal role in supplying newborn inhibitory interneurons to the OB and in ensuring its structural integrity and functionality [54, 57]. We tested if the increased proliferation and the cell cycle modification detected in the p21 KO mice after 12 days of physical activity impacted the migratory dynamics of post-mitotic neuroblasts. In order to verify this hypothesis, we treated the different experimental groups with five daily injections of BrdU (95 mg/kg) and sacrificed them 1 week after the last injection (Fig. 4a). This protocol allowed us to properly follow the differential migratory properties, along the caudal-rostro path SVZ-RMS-OB, of the BrdU+ newborn neuroblasts. However, this procedure was not applicable to the experimental group p21 KO run 21d,

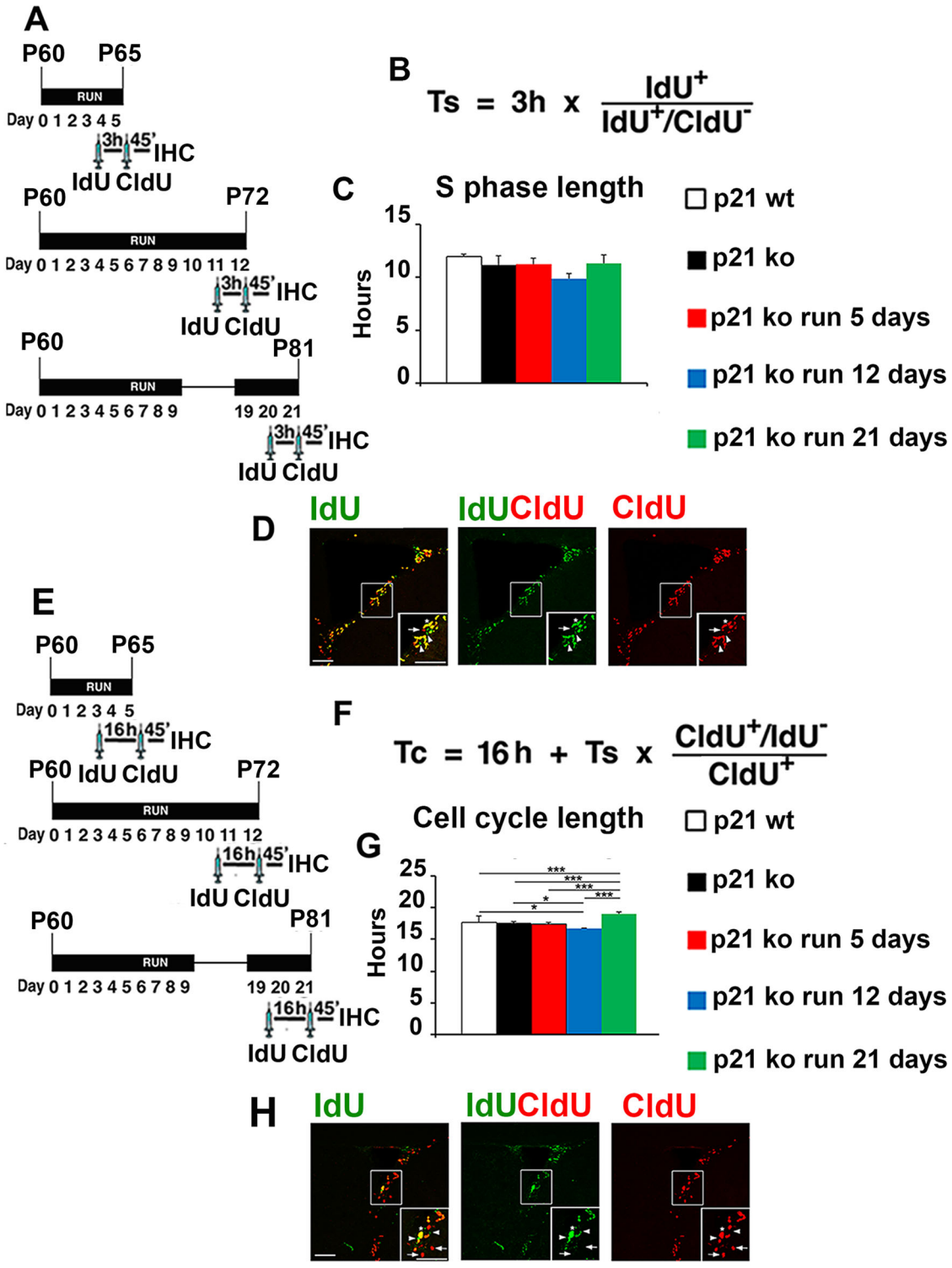

I

	p21 wt	p21 ko	p21 ko run 5d	p21ko run12d	p21ko run21d
TCycle	17,65 ± 0,20 h	17,64 ± 0,11 h	17,37 ± 0,34 h	16,77 ± 0,08 h	19,03 ± 0,34 h
Ts	9,48 ± 0,21 h	9,27 ± 0,55 h	9,89 ± 0,38 h	10,02 ± 0,27 h	10,77 ± 0,62 h
TG2/M	5 ± 0,01 h	5 ± 0,01 h	5 ± 0,01 h	5 ± 0,01 h	5 ± 0,01 h
TG1	3,37 ± 0,36 h	3,66 ± 0,53 h	2,68 ± 0,57 h	1,35 ± 0,27 h	3,46 ± 0,65 h

◀ **Fig. 3** Cell cycle length analysis reveals a running-dependent shortening of cell cycle length in p21 KO mice after 12 days of running. **a** Experimental timeline of the different pulses thymidine analogs for S-phase measurement. Mice were put in the running cage for 5, 12, or 21 days. On the last day of running, they received double pulses, separated by 3 h, of IdU and CldU, and were perfused after 45 min from the second injection (as explained in detail in "Material and Methods"). **b** Equation for the calculation of the S-phase length. The ratio of cells that have left the S-phase during the 3-h inter-injection interval ($IdU^+/CldU^-$ cells) to the total number of IdU+ cells is equal to 3 h/Ts. **c** Histogram illustrating S-phase length (in hours) among the five different experimental conditions. We did not find any significant differences among the five groups. **d** An interval of 3 h between IdU and CldU pulses produces three differentially labeled cell types: $IdU^+/CldU^-$ (green, arrowhead) which exited S-phase during the interval between the two pulses, IdU^-CldU^+ (red, arrow) which entered S-phase during the 3-h interval between the two injections, and $IdU^+/CldU^+$ double-labeled cells (yellow, asterisk) which were in the S-phase during both the injections (scale bar, 100 μm). **e** Experimental timeline of thymidine analogs injection for the precise calculation of the cell cycle length. In this case, the time interval between IdU and CldU was 16 h. **f** Equation for the calculation of the cell cycle with the IdU/CldU method. **g** Histogram illustrating the cell cycle calculation in the five experimental groups. Twelve days of running induces a significant decrease of cell cycle length in comparison with p21 WT and KO mice (p21 KO run 12d vs. p21 WT, $p < 0.05$ and p21 KO run 12d vs. p21 KO, $p < 0.05$). Finally, in the p21 KO run 21d mice, we observed a cell cycle lengthening compared with the other groups (p21 KO run 21d vs. p21 WT, $p < 0.001$ vs. p21 KO, $p < 0.001$). **h** An interval of 16 h between IdU and CldU injections produced cycling cells that were in the S-phase during the IdU injection only ($Idu^+/CldU^-$ cells, green, arrowhead), or during the CldU pulse ($IdU^-/CldU^+$ cells, red, arrow), or cells that re-entered the cell cycle and were in S-phase during both the pulse ($IdU^+/CldU^+$, yellow, asterisk; scale bar, 100 μm). **i** Table showing the length of the whole cell cycle, S-phase, G2/M phase, and G1 phase among the different experimental conditions. In the p21 KO run 12d, G1 phase was significantly shorter compared with the other groups except for p21 KO run 5d (p21 KO run 12d vs. p21 WT, $p = 0.015$, vs. p21 KO, $p < 0.01$ vs. p21 KO run 21d, $p < 0.01$). Cell number is mean ± SEM from the analysis of at least four animals *per* condition. Statistical significance: $*p < 0.05$, $**p < 0.01$, $***p < 0.001$. ANOVA analysis

which was consequently not taken into account in this study. The number of BrdU+ cells was measured in four different regions: SVZ (Fig. 4g), RMS (Fig. 4f), infrabulbar RMS (Fig. 4e), and OB (Fig. 4d), and their relative fraction in each area was determined from the sum of $BrdU^+$ cells counted in all the analyzed regions. We observed that the two sedentary conditions, p21 WT and p21 KO, did not display any noticeable difference in the $BrdU^+$ distribution (Fig. 4b, c, d), while in the p21 KO run 12d, a significantly higher percentage of $BrdU^+$ cells were located in the OB compared with all the other experimental conditions ($F_{(3,\ 29)} = 8.55$, $p < 0.001$, one-way ANOVA followed by Fisher's PLSD post hoc test; Fig. 4b, c, d). Moreover, we observed a diminished fraction of $BrdU^+$ cells in the SVZ of the p21 KO run 12d mice in respect to that measured in the sedentary p21 WT and KO mice ($F_{(3,\ 29)} = 3.02$, $p = 0.046$, one-way ANOVA followed by Fisher's PLSD post hoc test; Fig. 4b, c, f). Finally, we detected that in the WT animals, 5 and 12 days of physical activity did not induce any significant improvement in the migration rate of post-mitotic neuroblasts with respect to the sedentary littermates (data not shown).

These findings imply that the newly generated neuroblasts in the p21 KO mice migrate from the SVZ to their definitive destination at a significantly accelerated rate when exposed to voluntary wheel running for a period of 12 days, thus suggesting an accelerated differentiative rate of this population inside the OB. To test this hypothesis, we measured in the OB the total number of $BrdU^+NeuN^+$ cells as well as the percentage of differentiating new neurons (calculated as the ratio $BrdU^+NeuN^+$/total $BrdU^+$ cells in the OB), and we found that both this parameters significantly increased in the p21 KO run 12d in comparison with the other groups ($BrdU^+NeuN^+$ cells: $F_{(3,\ 31)} = 17.88$, $p < 0.001$, one-way ANOVA followed by Fisher's PLSD post hoc test, Fig. 4h; differentiating new neurons: $F_{(3,\ 31)} = 3.56$, $p < 0.05$, one-way ANOVA followed by Fisher's PLSD post hoc test, Fig. 4i). Overall, these data suggested that the concomitant deletion of p21 and the presence of a pro-neurogenic stimulus such as physical exercise are necessary and sufficient to induce a general increase, above physiological conditions, of the number of mature neurons in the OB as a consequence of the larger production of NSCs in the SVZ, of the faster post-mitotic neuroblast migration and of their increased differentiative rate.

Running Triggers Functional Activation of Newborn Neurons in the Olfactory Bulb of p21 KO Mice

In the OB, 4-weeks-old newly generated neurons are recruited in the olfactory circuits as GABA-ergic inhibitory modulators of mitral/tufted cells. The recruitment of OB newborn neurons is highly enhanced by olfactory stimulation [58], and the concomitant expression of BrdU and the immediate early gene c-fos is often used to analyze the functional activation of newborn neurons in the adult OB [44, 59]. Indeed, in order to explore whether the enhanced neurogenesis detected in the p21 KO run 12d mice resulted in the functional recruitment of newborn neurons, we treated the animals with five daily injections of BrdU and 4 weeks later, we exposed them to five presentations of the octanal odorant. The mice were sacrificed 1.5 h following olfactory stimulation in order to allow the expression of the c-fos protein (Fig. 5a). As a first step, we measured the total number of 4-weeks-old neurons which had incorporated BrdU and found that in p21 KO run 5d and 12d mice, the total number of $BrdU^+/NeuN^+$ cells within the OB was significantly higher in comparison with the p21 WT and p21 KO run 21d groups ($F_{(4,\ 70)} = 6.44$, $p < 0.001$, one-way ANOVA followed by Fisher's PLSD post hoc test; Fig. 5b). Moreover, when we analyzed the rate of functionally activated newborn neurons ($c\text{-}fos^+BrdU^+/BrdU^+$ total cells) after olfactory stimulation, we found that only those belonging to the p21 KO run 12d group showed an increment in respect to the

C

	p21wt vs p21ko	p21wt vs p21ko run 5d	p21wt vs p21ko run 12d	p21ko vs p21ko run 5d	p21ko vs p21ko run 12 d	p21ko run 5d vs p21ko run 12 d
SVZ	n.s.	n.s.	p = 0.014	n.s.	p = 0.019	n.s.
RMS	p = 0.009	p = 0.0006	p = 0.0004	n.s.	p = 0.039	n.s.
OB (RMS)	n.s.	n.s.	n.s.	n.s.	n.s.	n.s.
OB	n.s.	n.s.	p = 0.0001	n.s.	p = 0.0001	p = 0.0023

SVZ Subventricular zone; RMS Rostral MIgratory Stream; RMS (OB) intra bulbar RMS; OB Olfactory Bulb. n.s. not significant

B

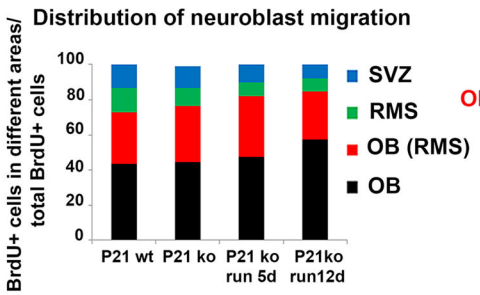

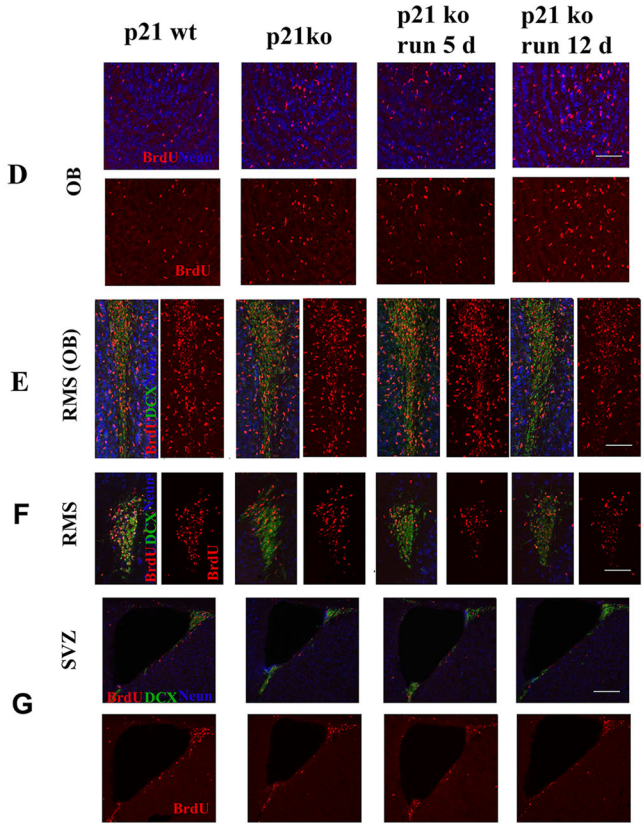

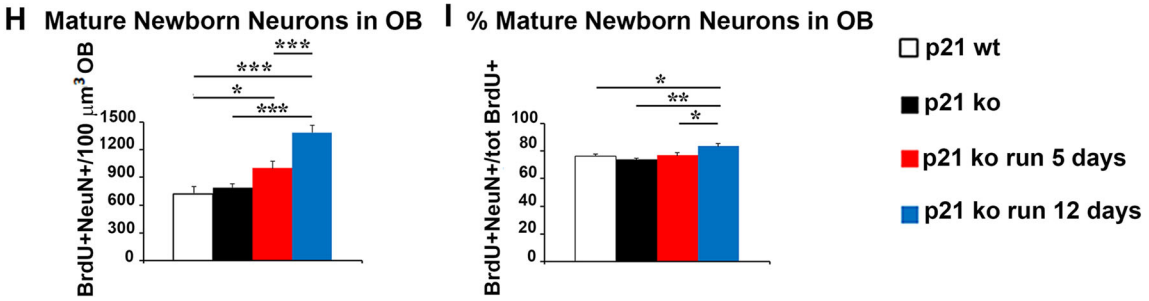

◀ **Fig. 4** Twelve days of running induced a faster migration of post-mitotic neuroblasts in p21 KO mice. **a** Experimental procedure of BrdU injections for the analysis of the migratory kinetic of post-mitotic neuroblasts. Mice groups (with the exception of p21 KO run 21d) received five daily pulses of BrdU and were then sacrificed 7 days after the last injection of BrdU. **b** The quantification of $BrdU^+/DCX^+$ cell distribution in different migratory stages indicates that running for 12 days accelerates migration of the newly generated neuroblasts. **d**–**g** Representative confocal images of coronal sections showing the migration path of neuroblasts from the SVZ (**d**), along the RMS (**e**), to the infra-bulbar RMS (**f**), and finally to the OB (**g**). Cells in the different regions were identified by triple-labelling with $BrdU^+/DCX^+/NeuN^+$ represented in red, green, and blue, respectively. The images show the accelerated migratory trend in the p21 KO run 12d mice with a smaller number of $BrdU^+$ cells in the SVZ and an increase in BrdU labelling in the OB compared with the other experimental conditions (scale bar, 75 μm). **h** Histogram showing the increase in the overall number of newborn neurons in the OB following physical exercise compared with physiological condition (p21 KO run 12d vs. p21 WT, $p < 0.001$, vs. p21 KO, $p < 0.001$, vs. p21 KO run 5d, $p < 0.001$). **i** Increase in the percentage of mature neurons over the total number of $BrdU^+$ cells in the OB in the p21 KO run 12d in comparison with WT mice (p21 KO run 12d vs. p21 WT, $p < 0.05$, vs. p21 KO, $p < 0.01$, vs. p21 KO run 5d, $p < 0.05$). Cell number is mean ± SEM from the analysis of at least four animals *per* condition. Statistical significance: $*p < 0.05$, $**p < 0.01$, $***p < 0.001$. ANOVA analysis

other experimental conditions ($F_{(4,\ 70)} = 11.5$, $p < 0.001$, one-way ANOVA followed by Fisher's PLSD post hoc test; Fig. 5c, d). These data further confirm that 12 days of running specifically triggered the pro-neurogenic potential of NSCs and improved the functional recruitment rate of newly generated neuroblasts lacking the inhibitory control exerted by p21.

Twelve Days of Running Improves Olfactory Behavior in p21 KO Mice

Several studies have described that adult SVZ neurogenesis profoundly affects some aspects of olfactory behavior, in particular the odor detection threshold which specifically measures the mouse's odor perception capacity, and the short-term olfactory memory [53, 54, 58]. We hypothesize that the enhanced SVZ neurogenesis and the increased functional activation of newborn neurons in the p21 KO run 12d mice might impact both olfactory behaviors.

As a first step, we analyzed spontaneous motor activity and anxiety level of p21 WT and KO mice, in the open field test. Our data showed that, while the distance traveled and the velocity were higher in p21 KO mice ($p < 0.05$ for both the parameters, *t* test analysis; Supp. Fig. 3 A, B), anxiety level was comparable between groups, as evaluated by the percentage of time spent in the center versus the periphery of the arena ($p > 0.05$, *t* test analysis; Supp. Fig. 3 C).

In the odor detection threshold test, mice were presented with a pair of cotton swabs soaked, respectively, with mineral oil and octyl-aldehyde odorant in increasing concentration (10^{-7}, 10^{-5}, 10^{-4}, 10^{-3}%) (Fig. 6a). In this test, a > 50% odor sniffing duration versus above mineral oil (assessed by a single sample *t* test analysis) reflects the animal's ability to detect the odor over the background [54]. p21 KO run 21d group was not included in these experiments due to the absence of any proneurogenic effect provided by this running paradigm. We observed that in the first day of the test (octyl-aldehyde concentration at 10^{-7}%), the time spent by p21 KO run 12d mice sniffing the odor over the mineral oil was noticeably longer (69% ± 1.41) than the other experimental groups («genotype × concentration» interaction, $F_{(9,\ 63)} = 10.53$, $p < 0.001$, two-way ANOVA followed by Fisher's PLSD post hoc test; Fig. 6b). These data suggest a specific improvement of sensitivity to very low concentrations of odors in the p21 KO run 12d mice. In the second and third days of testing (octyl-aldehyde concentration at 10^{-5}% and 10^{-4}%, respectively), we observed a gradual increase in the time interval spent in sniffing the odor by sedentary p21 WT and p21 KO run 5d mice, while the preference for the odorant of p21 KO run 12d mice decreased, likely because the odor was already familiar to the animals. Noteworthy, single sample *t* test analysis indicated that for p21 KO mice, sniffing at the odorant was never longer than sniffing the mineral oil (i.e., the odor detection index was never significantly > 50%), suggesting a low odor sensitivity likely dependent on the p21 deletion (Fig. 6b). Similar results were attained when butyl-butyrate was used (Fig. 6c).

To assess the concomitant effect of p21 deletion and running on the short-term olfactory memory, 4 weeks after physical exercise, the mice were submitted to an olfactory task, in which they were exposed twice to the same odorant at different time intervals (Fig. 6d). The difference in the duration of sniffing between the first and the second exposures was considered as an indication of olfactory memory. We tested the animals at four different time intervals (30, 240, 300, 360 min) using a different odorant each time. p21 KO mice were excluded from the experiment due to their scarce odor sensitivity. Our data showed that the p21 WT, p21 KO run 5d, and p21 KO run 12d maintained a robust memory of the odor at 30, 240, and 300 min (Fig. 6e–g). However, only the p21 KO run 12d mice showed olfactory memory when tested 360 min after the first exposure, while the other groups did not (Student's *t* test, $p < 0.05$, first vs. second exposure; Fig. 6g). This result indicates that the enhanced maturation of newborn neurons in the OB could be related to the improvement of the short-term olfactory memory in the p21 KO run 12d mice. As for the odor detection threshold, it is worth to note that the effect of running is magnified by the concomitant loss of the p21 gene.

Physical Activity Induces In Vitro Expansion of p21-Null Neural Stem Cells

We then asked how physical activity might affect the type of division (symmetric vs. asymmetric) of the NSCs within the

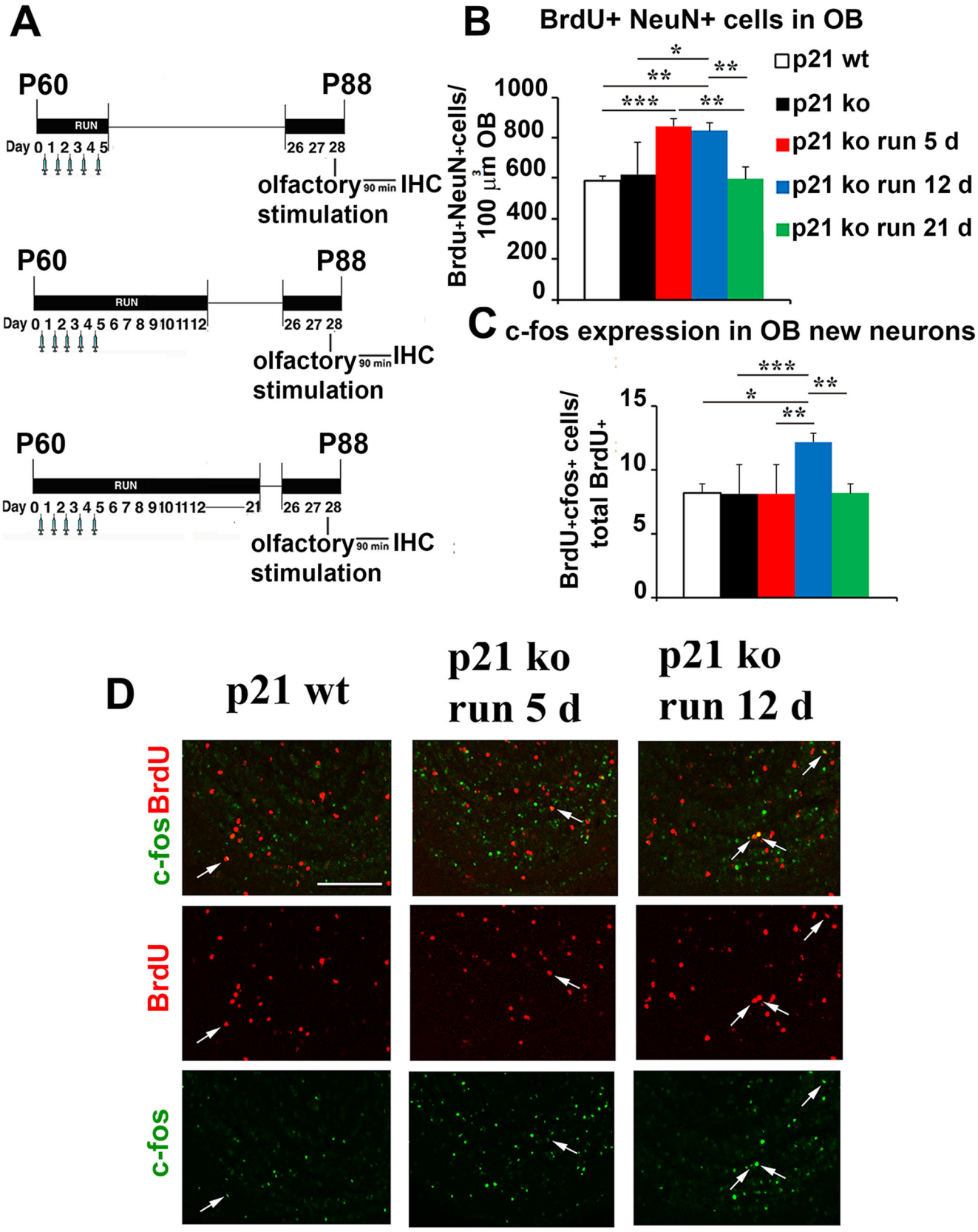
A
P60
P88
RUN
Day 0 1 2 3 4 5
26 27 28
olfactory stimulation
90 min
IHC
P60
P88
RUN
Day 0 1 2 3 4 5 6 7 8 9 10 11 12
26 27 28
olfactory stimulation
90 min
IHC
P60
P88
RUN
Day 0 1 2 3 4 5 6 7 8 9 10 11 12 21
26 27 28
olfactory stimulation
90 min
IHC
B
BrdU+ NeuN+ cells in OB
Brdu+NeuN+cells/ 100 μm3 OB
1000
800
600
400
200
0
*
**
**
***
**
p21 wt
p21 ko
p21 ko run 5 d
p21 ko run 12 d
p21 ko run 21 d
C
c-fos expression in OB new neurons
BrdU+cfos+ cells/ total BrdU+
15
10
5
0
***
*
**
**
D
p21 wt
p21 ko run 5 d
p21 ko run 12 d
c-fos BrdU
BrdU
c-fos

◀ **Fig. 5** Twelve days of running improves functional recruitment of newborn neurons after olfactory stimulation in p21 KO mice. **a** Different protocols for BrdU injections in the three running paradigms. **b** Total amount of $BrdU^+NeuN^+$ cells observed in the OB, significantly increased 5 and 12 days running p21 KO groups in comparison with p21 WT and KO sedentary mice (p21 WT vs. p21 KO run 5d, $p < 0.001$, vs. p21 KO run 12d, $p < 0.01$). **c** Graph illustrating that the total number of activated newborn neurons in the OB increases in 12 days running p21 KO mice compared with the other groups (p21 KO run 12d vs. p21 WT, $p < 0.001$, vs. p21 KO, $p < 0.001$, vs. p21 KO run 5d, $p < 0.001$, vs. p21 KO run 21d, $p < 0.001$). **d** Representative confocal images of coronal sections of the olfactory bulb showing the functional integration of newborn neurons in p21 WT and p21 KO mice after running for 5 and 12 days. They are identified as double-labeled $BrdU^+$/$c\text{-}fos^+$ represented in red and green, respectively (scale bar, 100 μm). Cell number is mean ± SEM from the analysis of at least four animals *per* condition. Statistical significance: $*p < 0.05$, $**p < 0.01$, $***p < 0.001$. ANOVA analysis

SVZ of 2-month-old p21 KO mice. To address this issue, we performed neurosphere (NS) cultures by SVZ-derived NSCs in the five experimental conditions. In this in vitro model of NSC proliferation, symmetric divisions contribute to produce more NS, increasing the pool of NSCs, while asymmetric divisions result in an increase of the volume of the NS [55]. To isolate and characterize the NSCs in the SVZ, p21 WT and KO mice were crossed with Nestin-GFP mice [48], in which GFP expression is driven by the promoter of the NSC-specific gene Nestin. GFP^+ NSCs were isolated by fluorescent-activated sorting (FACS; Fig. 7a) from the SVZ of p21 WT/NestinGFP mice (referred as p21 WT/GFP mice), p21 KO/GFP mice, and p21 KO/GFP mice after 5, 12, and 21 days of running. At the first passage (7 DIV), we observed that p21 loss induced an increase both in the number (reflecting more symmetric divisions) and in the size (reflecting more asymmetrical divisions) of GFP^+ primary NSFs, as compared with control p21 WT/GFP mice (number of NSFs: $F_{(4,\ 10)} = 157.41$, $p < 0.001$, one-way ANOVA followed by Fisher's PLSD post hoc test; volume of NSFs: $F_{(4,\ 53)} = 7.713$, $p < 0.001$, one-way ANOVA followed by Fisher's PLSD post hoc test; Fig. 7b, c, d). Interestingly, the number and the size of secondary NSFs derived from p21 KO/GFP (14 DIV) mice reached values comparable to those measured in WT (number of NSFs: $F_{(3,\ 8)} = 12.166$, $p < 0.01$, one-way ANOVA followed by Fisher's PLSD post hoc test; volume of NSFs: $F_{(3,\ 81)} = 6.640$, $p < 0.001$, one-way ANOVA followed by Fisher's PLSD post hoc test; Fig. 7b, c, d). Remarkably, 5 days of running induced a significant increase in the number of secondary p21 KO GFP^+ NSFs ($F_{(3,\ 8)} = 12.166$, $p = 0.002$, one-way ANOVA followed by Fisher's PLSD post hoc test; Fig. 7e), while 12 days of running resulted in a striking enhancement in GFP^+ NSFs volume and in proliferative index with respect to the other conditions (proliferative index: $F_{(3,\ 8)} = 61.94$, $p < 0.001$, one-way ANOVA followed by Fisher's PLSD post hoc test; Fig. 7f, g). Instead, we did not obtain any GFP^+ NS from p21 KO/GFP mice after 21 days of running, suggesting that these cells quickly lose their stemness potential once cultured in vitro. At the fourth passage (28 DIV), the reduced capabilities of forming NSFs of p21 KO/GFP NSCs became more evident (Fig. 7h, i, j), confirming previous data indicating that p21 deletion induced a progressive decline of both self-renewal and proliferative capacity of NSCs in vitro [54]. At this stage, we observed a similar trend detected in the NSFs at DIV14, with 5 days of running resulting in a large enhancement of the number of p21-null NSFs ($F_{(3,\ 8)} = 100.94$, $p < 0.001$, one-way ANOVA followed by Fisher's PLSD post hoc test; Fig. 7h, i), while 12 days of running induces a concomitant enhancement of number and size of NSFs, largely exceeding the physiological values (volume of NSFs: $F_{(3,\ 90)} = 36.214$, $p < 0.001$, one-way ANOVA followed by Fisher's PLSD post hoc test; Fig. 7h, i, j). The in vitro results confirm that, in p21 KO mice, physical activity increases neurogenesis by inducing NSC self-renewal (through symmetric division) and, subsequently, differentiation (through asymmetric division). This led us to hypothesize that 12 days of running give rise to a hyper-activated NSCs population, able to significantly increase SVZ neurogenesis and the olfactory behavior of p21 KO mice at 2 months of age.

Proneurogenic Effect of Running in 12-Month-Old SVZ of p21 KO Mice

It has been extensively demonstrated that in aging, the constitutive deletion of the p21 gene induces a striking reduction of hippocampal and SVZ neurogenesis mainly due to the progressive exhaustion of the NSC pool and, to a lesser extent, to the increase of replicative stress in neural progenitors [32, 55]. To verify if physical activity is able to not only counteract the age-dependent exhaustion of NSC pool but also to reactivate SVZ neurogenesis in the p21 KO aged mice, 12-month-old mice were subjected to the same running experimental conditions as P60 mice. In accordance with previous results, the SVZ of p21 KO mice displayed a significant decrease of cell proliferation ($Ki67^+$ cells: $F_{(4,\ 116)} = 15.234$, $p < 0.001$, one-way ANOVA followed by Fisher's PLSD post hoc test; Fig. 8a, e–i), and of the number of type B cells in comparison with the p21 WT mice ($GFAP^+$/$SOX2^+$ cells: $F_{(4,\ 55)} = 10.125$, $p < 0.001$, one-way ANOVA followed by Fisher's PLSD post hoc test; Fig. 8b, e–i). However, we did not observe a similar reduction when we analyzed the recruitment and expansion rate of type B cells (Fig. 8c, d). We also noted a sharp reduction of type B/type C ($Nestin^+$ cells: $F_{(4,\ 50)} = 8.33$, $p = 0.00003$, one-way ANOVA followed by Fisher's PLSD post hoc test; Supp. Fig. 4 A, E-I) and type A cells in the p21-null mice with respect to the WT counterpart (DCX^+ cells: $F_{(4,\ 51)} = 11.041$, $p < 0.001$, one-way ANOVA followed by Fisher's PLSD post hoc test; Supp. Fig. 4 B, E-I). In the p21 KO mice, we observe that only the short-term paradigm of running (5 days) was able to trigger a large increase of type

B recruitment ($F_{(4,\ 55)} = 5.974$, $p < 0.001$, one-way ANOVA followed by Fisher's PLSD post hoc test; Fig. 8c, e–i) and expansion (expressed as the $Ki67^+SOX^+GFAP^+$ cell density), largely exceeding the values measured in WT mice ($F_{(4,\ 55)} = 8.602$, $p < 0.001$, one-way ANOVA followed by Fisher's PLSD post hoc test; Fig. 8d, e–i). These events evolved in a dramatic increase of the overall proliferation ($Ki67^+$ cells) of newborn cells in the p21 KO run 5d old mice, which reached values well above those observed in all the other experimental mice groups ($F_{(4,\ 116)} = 15.234$, $p < 0.001$, one-way ANOVA followed by Fisher's PLSD post hoc test; Fig. 8a, e–i). Moreover, we observed that 5 days of running induced in the p21 KO mice a significant enhancement of the proliferating fraction of type B/C cells and type A neuroblasts in respect to the WT mice ($Ki67^+Nestin^+$ cells, $F_{(4,\ 50)} = 22.63$, $p < 0.001$, one-way ANOVA followed by Fisher's PLSD post hoc test; Supp. Fig. 4 C; $Ki67^+DCX^+$ cells, $F_{(4,\ 51)} = 8.24$, $p < 0.001$, one-way ANOVA followed by Fisher's PLSD post

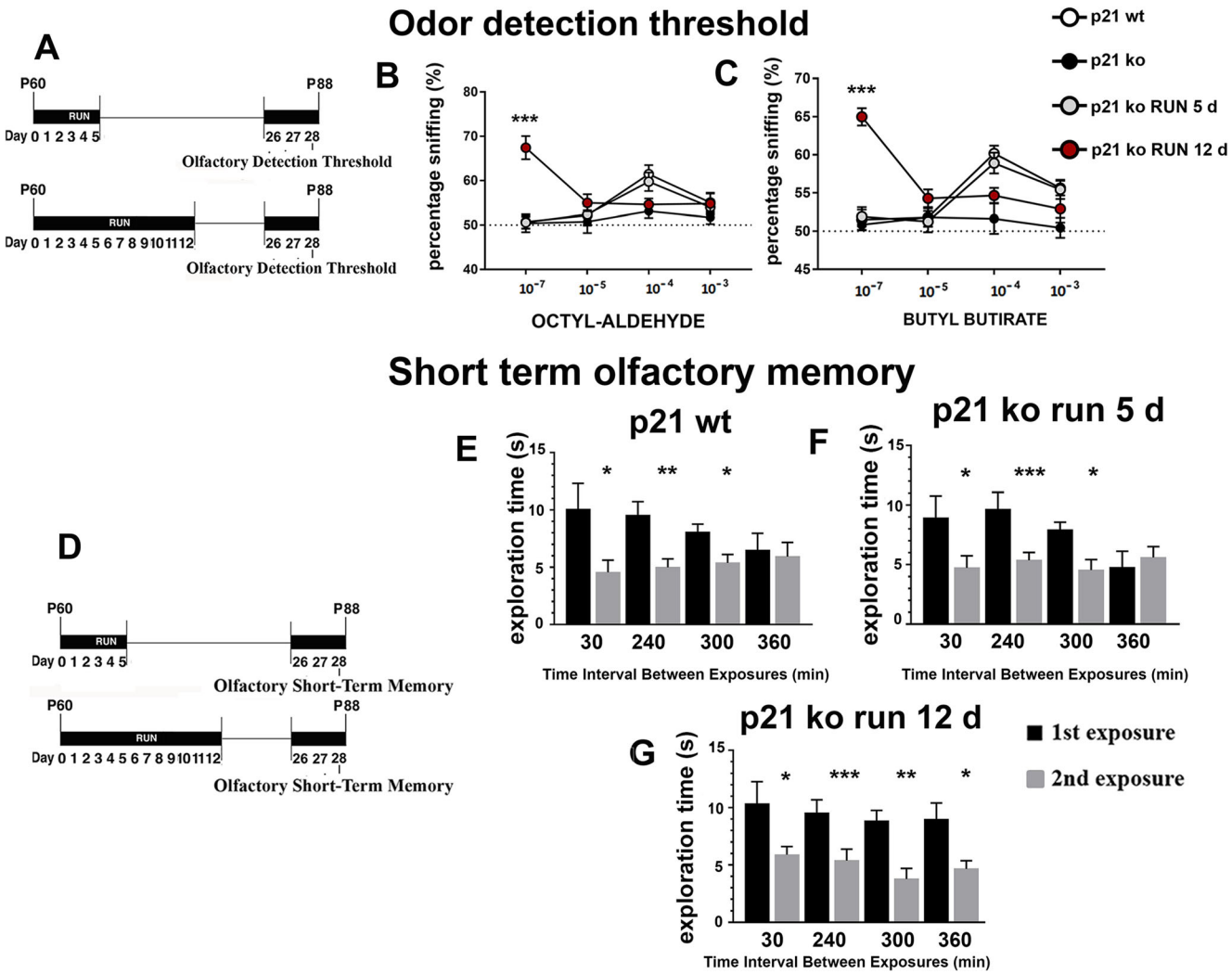

Fig. 6 Improved olfactory detection in p21 KO mice after 12 days of running. **a** Experimental design for the odor detection test. **b** p21 KO run 12d mice were able to detect octyl-aldehyde at a concentration of 10^{-7}%, while both WT mice and p21 KO run 5d mice only detected the odor at a concentration of 10^{-4}%. p21 KO mice did not detect the odor, not even at the highest concentration of 10^{-3}% («genotype × concentration» interaction, p21 KO run 12d vs. p21 WT, p21 KO and p21 KO run, $p < 0.001$). Values are expressed as the percentage of time the animals spent sniffing at the target odorant on the total time they spent sniffing (at both the odor sources). **c** Odor detection threshold to butyl-butyrate. Also in this case, p21 KO run 12d mice showed to be able to detect the odor even at the lowest concentration of 10^{-7}%, undetectable to all the other groups («genotype × concentration» interaction, $F_{(9,\ 75)} = 2.11$, $p < 0.001$, two-way ANOVA followed by Fisher's PLSD post hoc test, p21 KO run 12d vs. p21 WT, p21 KO and p21 KO run, $p < 0.001$). A > 50% sniffing duration (above chance) indicates odorant detection. **d** Experimental design for the short-term olfactory memory test. **e**–**g** Each bar of the graph represents the time animals spent investigating a given odor on the first (black columns) and the second (white columns) exposure. p21 WT and p21 KO run 5d mice showed intact memory for the odor 30, 240, and 300 min after the first exposure; however, the p21 KO run 12d mice were able to remember the odor after 360 min (Student's *t* test, $*p < 0.05$, $**p < 0.01$, $***p < 0.001$, first vs. second exposure). $N = 7$–8 mice/group

hoc test; Supp. Fig. 4 D), which contribute to recover the diminished number of types C and A progenitor sub-populations observed in the sedentary p21 KO mice. It is important to note that at this age, 12 and 21 days of running did not exert any beneficial role in increasing SVZ neurogenesis in the p21 KO mice (Supp. Fig. 4, A-D). Our data suggested that aged NSCs lacking the cell cycle inhibitor p21 still maintain a high proneurogenic potential in terms of recruitment, expansion, and proliferation, when stimulated by an external stimulus such as physical exercise.

Discussion

In the present study, we examined the effect of voluntary physical activity on SVZ neurogenesis of p21-null mice. Our data provides original findings showing that in the absence of the p21 gene, SVZ neurogenesis and olfactory behavior are significantly enhanced by voluntary running. We demonstrated that the main event triggering an increased SVZ neurogenesis in p21 KO running mice is represented by an enhanced rate in the recruitment of quiescent NSCs in the cell cycle, leading to a consistent increase in the expansion capacity of the p21-lacking NSCs and in the NSC pool available for the following proliferative/differentiative steps within the SVZ. We have also demonstrated that voluntary physical exercise in the p21-null mouse model accelerates the migration of post-mitotic neuroblasts toward the OB, which entails an elevated maturation rate and an enhancement in the functional integration of newborn neurons within the olfactory bulb circuits following olfactory stimulation. Moreover, behavioral tests clearly demonstrate that p21 KO mice show a better performance in the odor detection threshold short-term olfactory memory after 12 days of voluntary running. Finally, our results demonstrated that in 12-month-old mice, 5 days of running are still able to rescue the declined SVZ neurogenesis detected in p21 KO mice, far exceeding the physiological levels. These findings indicate that p21-null SVZ NSCs maintained a pro-neurogenic potential throughout the lifespan and that the declined adult neurogenesis in p21 knockout mice can be strongly upregulated above physiological levels by a short-medium input of physical activity. Supporting our hypothesis, a recent paper has shown that the conditional expression of the CCDK4/cyclinD1 complex is able to expand the pool of NSCs within the SVZ, to increase the number of new neurons in the olfactory bulb, and finally to improve the olfactory discrimination of mice when tested with a challenging task [60].

The role exerted by p21 in maintaining the homeostasis in the adult neurogenic niches has been extensively analyzed by the use of the constitutive p21 knockout mouse model. These investigations showed that deletion of p21 induces an expansion of the NSCs due to a large increase of symmetric and asymmetric divisions [54], resulting in a progressive exhaustion of the self-renewal capacities and to a consistent decline of hippocampal and subventricular neurogenesis [28, 29, 32, 33]. However, such a decrease is still not apparent in vivo at 2 months of age [31, 55], while in vitro experiments have shown a significant enhancement in self-renewal and expansion of p21-null NSCs at this stage, leading to the hypothesis that the enhanced proliferation occurred exclusively on the relatively small sub-population of type B cells [31, 32].

In our experiments, we did not find evidence of any increase in the pool size nor in the proliferating p21-devoid NSCs of 2-month-old mice, whereas, in agreement with previous studies, the decline of SVZ neurogenesis is quite evident in p21 KO mice at 12 months of age. In the young p21 KO mice, the only significant difference that we noticed in respect to the control condition is represented by the increase in SOX2 expression. These observations confirm other data showing how p21 maintains the proper regulation of the cell cycle transition in NSCs by binding the enhancer sequence and by repressing the expression of the SOX2 gene, which represents one of the main transcription factors of stem pluripotency. Remarkably, the long-term increase of SOX2 expression in the adult SVZ induces cell cycle arrest, replicative stress, and the onset of DNA damage in hyper-proliferating p21-null NSCs and progenitor cells [33]. We speculate that a similar process might occur in the NSCs of the p21 KO mice after 21 days of running. In fact, we observed a progressive increase of SOX2 expression in 5 and 12 days running p21 KO mice that could induce replicative stress and cell cycle arrest in the course of the longer running paradigm, with the result that after 21 days of running the pro-neurogenic effects exerted by physical exercise are completely abolished.

In this research, we provide clear indications that in 2-month-old p21 KO mice, 12 days of running induced the most powerful pro-neurogenic stimulus for activation, proliferation, migration, maturation, and functional integration of new neurons in the SVZ-OB axis neurogenesis. In contrast, a 5-day running protocol plays a positive role only in the first proliferative steps occurring in the SVZ of p21 KO mice. Our data led us to hypothesize that in the p21 KO mouse, running establishes a series of cellular modifications (cell cycle shortening, increase of NSC pool size, and enhanced proliferation) which could require a well-defined timing to optimize their pro-neurogenic action. In this regard, in vitro data suggest the existence of a multi-step mechanism strictly correlated with the pro-neurogenic effect of physical activity in the p21 KO mice. Indeed, we observed that a short-term running session (5 days) was able to expand the NSC pool likely through the increase of neurogenic symmetrical division, while a medium-term running session (12 days) further triggered a significant enhancement of asymmetric differentiative divisions leading to a large production of neural progenitors. Once the plateau of the pro-neurogenic effects has been reached, the beneficial

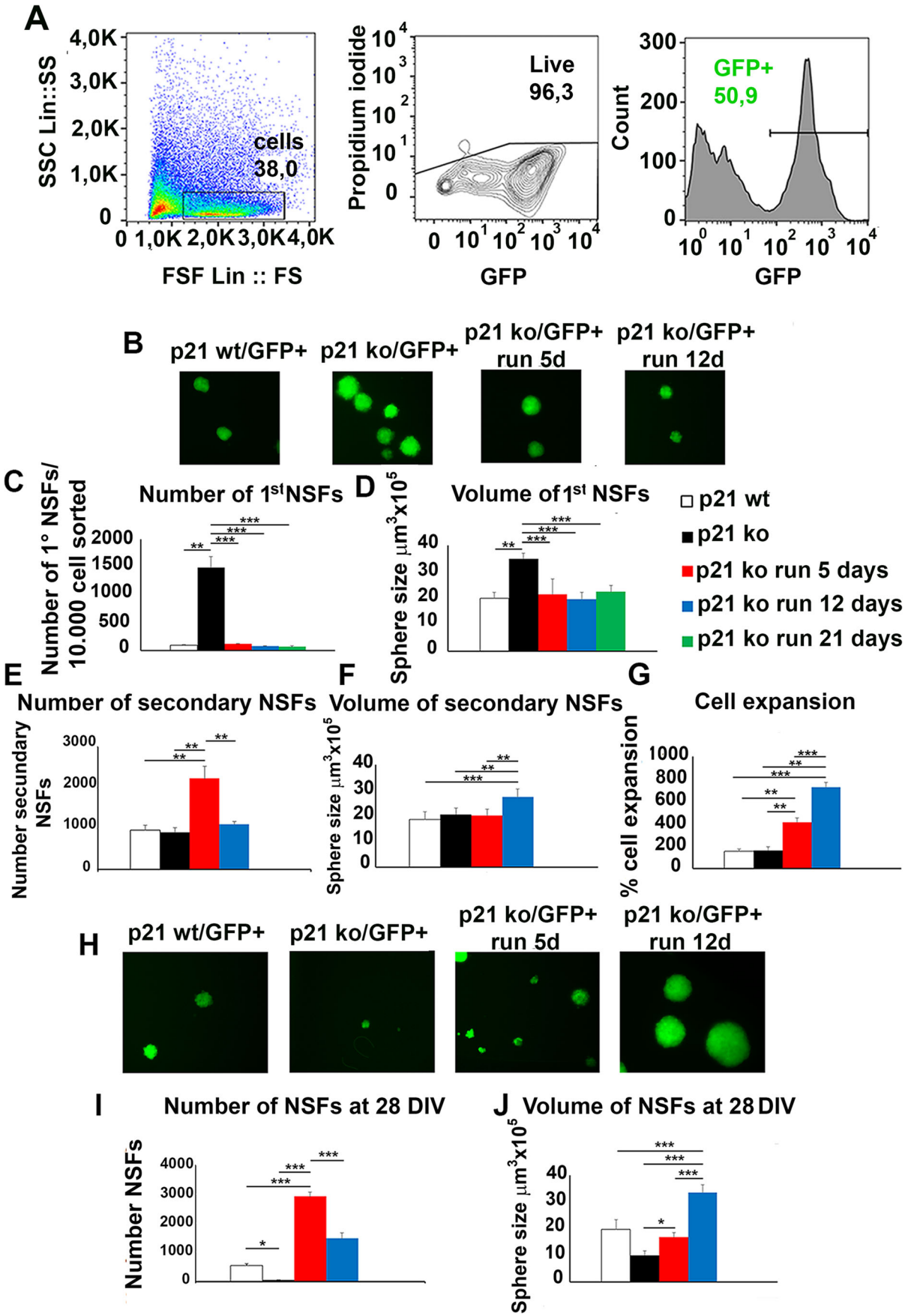
A
SSC Lin::SS
FSF Lin :: FS
cells
38,0
Propidium iodide
GFP
Live
96,3
Count
GFP+
50,9
B
p21 wt/GFP+
p21 ko/GFP+
p21 ko/GFP+ run 5d
p21 ko/GFP+ run 12d
C
Number of 1° NSFs/ 10.000 cell sorted
Number of 1st NSFs
D
Volume of 1st NSFs
Sphere size µm3x10^5
p21 wt
p21 ko
p21 ko run 5 days
p21 ko run 12 days
p21 ko run 21 days
E
Number of secondary NSFs
Number secundary NSFs
F
Volume of secondary NSFs
Sphere size µm3x10^5
G
Cell expansion
% cell expansion
H
p21 wt/GFP+
p21 ko/GFP+
p21 ko/GFP+ run 5d
p21 ko/GFP+ run 12d
I
Number of NSFs at 28 DIV
Number NSFs
J
Volume of NSFs at 28 DIV
Sphere size µm3x10^5

◀ **Fig. 7** Physical activity induces in vitro expansion and self-renewal of p21-null NSC pool. **a** Gating strategy to identify and sort cells of interest. Samples were stained with PI to exclude dead cells, and GFP+ cells were sorted in tubes. **b** Representative images of primary neurospheres (NSFs) derived from 2-month-old P21 WT/GFP$^+$ mice, p21 KO/GFP$^+$ mice, and p21 KO/GFP$^+$ mice after 5 and 12 days of running, showing the consistent increase in the number and size of GFP$^+$ NSFs isolated by FACS from p21 KO/GFP$^+$ mice. **c**, **d** Histograms showing the large increase in the number and size of primary GFP$^+$ NSFs (per 10.000 GFP$^+$ cells isolated by FACS) derived from the SVZ of p21 KO/GFP$^+$ mice (number of NSFs: p21 KO vs. p21 WT, vs. p21 KO run 5d, 12d, and 21d, $p < 0.0001$; volume of NSFs: p21 KO vs. p21 WT, $p < 0.05$, vs. p21 KO run 5d, 12d, and 21d, $p < 0.001$). **e**, **f** Histograms showing the number and size of secondary GFP$^+$ NSFs (per 10.000 GFP$^+$ cells plated, DIV 14), with a large enhancement of number and size of GFP$^+$ NSFs derived from p21 KO/GFP$^+$ run 5 and 12 days, respectively (number of NSFs: p21 KO run 5d vs. p21 WT, p21 KO and p21 KO run 12d, $p < 0.001$; volume of NSFs: p21 KO run 12d vs. p21 WT, $p < 0.001$, vs. p21 KO, $p < 0.01$, vs. p21 KO run 5d, $p < 0.001$). **g** Percentage of cell expansion of primary GFP$^+$ NSFs expressed as the total number of cells at the end of the culture at the second passage divided by the initial number of cells. Compared with the other conditions, a consistent expansion in the p21 KO/GFP$^+$ run 12d occurred (p21 KO run 12d vs. p21 WT, $p < 0.001$, vs. p21 KO, $p < 0.001$, vs. p21 KO run 5d, $p < 0.001$). **h** Representative images of GFP$^+$ NSFs after 28 days in vitro showing the large increase in the number of GFP$^+$ NSFs in the p21 KO/GFP$^+$ run 5d and of the GFP$^+$ NSFs volume in the p21 KO/GFP$^+$ run 12d. **i** Graphs showing the number of GFP$^+$ NSFs at 28 DIV (per 10.000 GFP$^+$ cells plated), in which we found a large increase in the p21 KO/GFP$^+$ after 5 and 12 days of running (p21 KO run 5d vs. p21 WT, $p < 0.$ 001, vs. p21 KO, $p < 0.001$, vs. p21 KO run 12d, $p < 0.$ 001). **j** Histogram showing the increased volume of GFP$^+$ NSFs at 28 DIV observed in the p21 KO/GFP$^+$ run 12d, in comparison with the other experimental groups (p21 KO run 12d vs. p21 WT, p21 KO and p21 KO run 5d, $p < 0.001$). Neurosphere parameters are expressed as mean ± SEM from the analysis of four animals per condition. Statistical significance: $*p < 0.05$, $**p < 0.01$, $***p < 0.001$. ANOVA analysis

role of running progressively loses its effectiveness, observed with the occurrence of the anti-neurogenic changes evident in the 21-day running protocol. This fact is even clearer when we analyzed the p21 KO mice at 12 months of age, in which the declined neurogenesis is fully recovered only by the short 5-day running session, while 12 and 21 days of physical exercise have no effect.

The results revealed that the main event triggering the increase of subventricular neurogenesis in 2-month-old p21 KO mice after 12 days of running is represented by the modification of the cell cycle kinetic. The 12-day running paradigm is able to induce in the SVZ of p21-null mice: (i) a shortening of the G1 phase and consequently of the entire cell cycle and (ii) a significant increase of cell cycle re-entry compared with the other experimental conditions. These events are of pivotal importance in allowing the p21-null neural progenitors to perform a greater number of divisions for a prolonged period of time, ensuring a great expansion of the SVZ sub-populations. To this regard, Calegari recently hypothesized that the length of the G1 phase plays a decisive role in the orchestration of the rate and the type (symmetric or asymmetric) of NSC division and that in turn the factors regulating the G1 phase influence this pattern. In short, a fast G1 is predictive for an expansion of stem cells, while its elongation is linked to differentiating events [61]. Consequently, the overexpression of the cyclin D1/CDK4 complex (referred as 4D), which is involved in the shortening of the G1 phase and in facilitating the G1/S progression, induces an expansion of NSCs both in the course of embryonic and adult neurogenesis without an obvious depletion of the NSC pool [62, 63]. According to the hypothesis, we observed a significant increase of cyclin D1 expression in p21 KO mice after 12 days of running (data not shown) which could be possibly related, via the shortening of the G1 phase, to the expansion of type B cells and the induction of lineage progression to neuroblasts.

Another mechanism involved in the transition between expansion and cell cycle arrest is the regulation of the re-entry of NSCs in the cell cycle. The importance of p21 in regulating this process has been highlighted in numerous studies showing how the deletion of several pro-neurogenic transcription factors during embryonic neurogenesis, such as Bmi-1 [64], Tlx [65], Pitx2 [66], and Dux4 [67], induces an increase in p21 expression; these events in turn lead to an early exit of cells from the cell cycle and to the repression of NSC expansion, further confirming the antiproliferative role of this gene. In our study, we demonstrated how 12 days of running is responsible for a significant increase of cell cycle re-entry of the SVZ p21-lacking neural progenitors. Moreover, we observed that the long-term paradigm of running (21 days) exerts its anti-neurogenic action in p21 KO mice even inducing a significant increase in cells exiting the cycle compared with the other two running protocols. Overall, the analysis of the cell cycle in the SVZ of p21 KO mice confirms that the length of the G1 phase is a prominent factor for the neurogenic action of physical exercise.

We also found a causal correlation between enhanced adult SVZ neurogenesis in the p21 KO run 12d mice and olfactory functions. Indeed, we demonstrated that in the p21 KO mice, 12 days of exercise increased the number of adult-born interneurons in the OB by promoting neuronal differentiation, maturation, and functional recruitment of adult born cells. These events contribute significantly to a greater supply of functionally active interneurons in the OB which guarantee greater synaptic plasticity and a more efficient flexibility in the odor-associated learning process with a resulting significant improvement in two odor tasks which have previously demonstrated to be strictly dependent on the continuous supply of newborn neurons to the OB: the odor detection threshold and the olfactory short-term memory [53, 54]. Accordingly, it has been shown that the constant arrival of newborn interneurons sustains structural and functional plasticities in the OB circuitry by allowing the correct turnover/addition of the OB interneuronal population [57, 68] and the execution of specific odor-associated behavior tasks. Moreover, it has been shown that new granule cells play a distinct role in plastic change

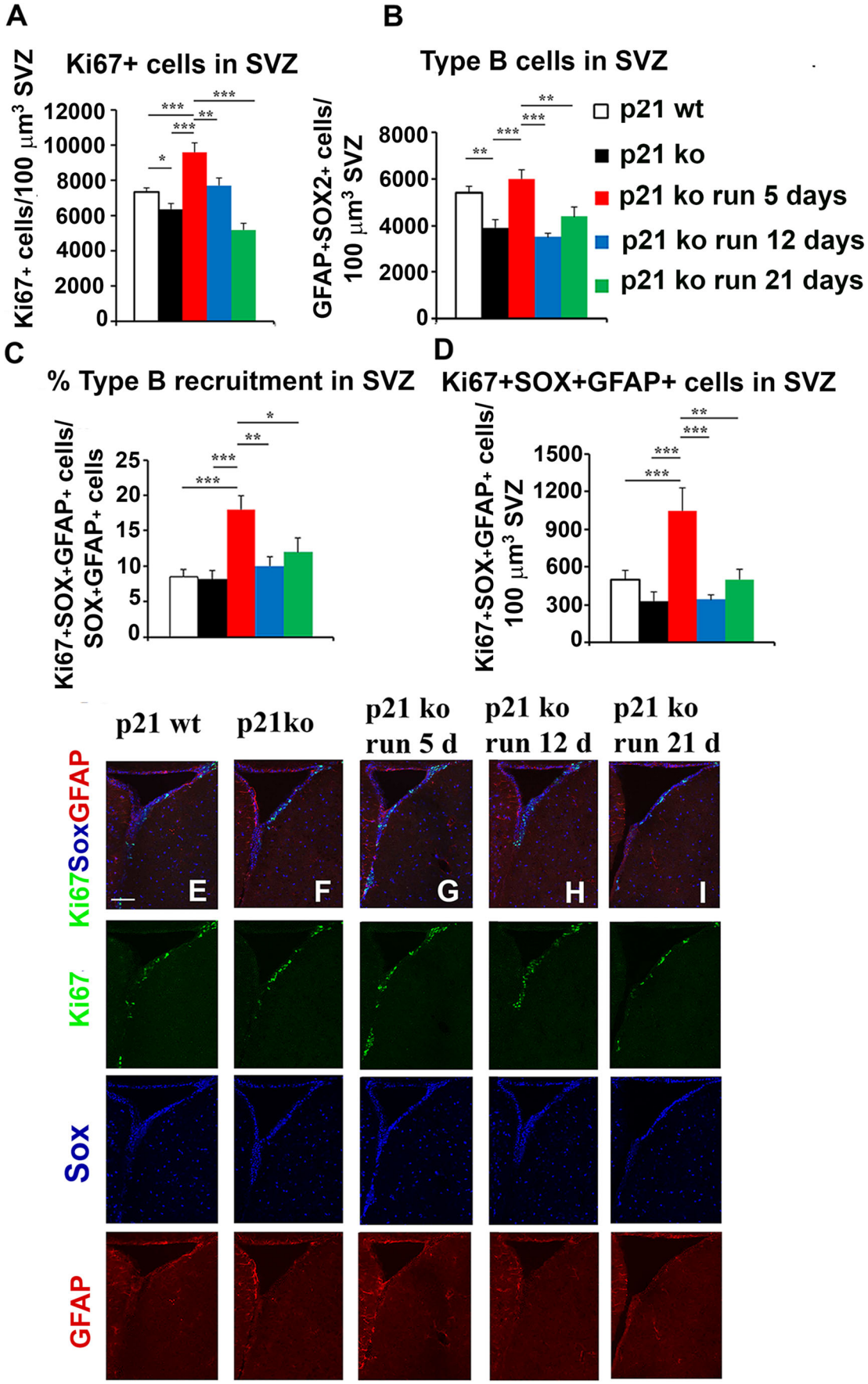
A
Ki67+ cells in SVZ
Ki67+ cells/100 μm³ SVZ
12000
10000
8000
6000
4000
2000
0
B
Type B cells in SVZ
GFAP+SOX2+ cells/ 100 μm³ SVZ
8000
6000
4000
2000
0
p21 wt
p21 ko
p21 ko run 5 days
p21 ko run 12 days
p21 ko run 21 days
C
% Type B recruitment in SVZ
Ki67+SOX+GFAP+ cells/ SOX+GFAP+ cells
25
20
15
10
5
0
D
Ki67+SOX+GFAP+ cells in SVZ
Ki67+SOX+GFAP+ cells/ 100 μm³ SVZ
1500
1200
900
600
300
0
p21 wt
p21ko
p21 ko run 5 d
p21 ko run 12 d
p21 ko run 21 d
Ki67SoxGFAP
Ki67
Sox
GFAP
E
F
G
H
I

◀ **Fig. 8** Effects of running on NSC recruitment and expansion in 12-month-old p21 KO mice. **a** Overall number of proliferating cells was significantly decreased in p21 KO mice compared with p21 WT mice. Running for 5 days induces in the p21 KO mice a significant increase of proliferation in comparison with the other mice groups (p21 KO run 5d vs. p21 WT, $p = 0.000012$). **b** In the p21 KO mice, the depleted type B ($GFAP^+/SOX2^+$ cells) pool size is reactivated by 5 days of running. **c** Histogram showing the percentage of type B cells recruited from quiescence (ratio between $KI67^+/SOX2^+/GFAP^+$ and total $SOX2^+/GFAP^+$ cells), increased in p21 KO run 5d mice compared with the other experimental groups (p21 KO run 5d vs. p21 WT, $p < 0.001$). **d** Increase in the number of dividing type B cells in the SVZ of p21 KO mice after 5 days of physical exercise (p21 KO run 5d vs. p21 WT, $p < 0.001$). **e**–**i** Representative confocal images of coronal sections showing the overall quantity of proliferating type B cells in the SVZ of 12-month-old mice, identified by triple-labelling of $Ki67^+/GFAP^+/SOX2^+$ (green, red, and blue, respectively) with the large increase of type B NSCs in p21 KO run 5d mice (scale bar, 100 μm). Cell density (cell number/volume SVZ) is mean ± SEM from the analysis of at least four animals per condition. Statistical significance: $*p < 0.05$, $**p < 0.01$, $***p < 0.001$. ANOVA analysis

within the OB, which is different from that of pre-existing neurons, suggesting a causal relationship between the activity of SVZ newly generated neurons and the specific function of the OB circuitry [8]. As proof of this, a series of studies have shown how mice with reduced SVZ neurogenesis exhibited alterations in fine olfactory discrimination and short-term memory [53, 69, 70], while rodents with genetically enhanced SVZ neurogenesis [54] or exposed to an enriched environment [18] and to extremely low-frequency electromagnetic fields [71] displayed a consistent improvement in olfactory behavior.

Finally, in the p21 KO aged mice, the massive decrease of NSC pool size and the consequent reduction of neural progenitor proliferation induced a dramatic drop of SVZ neurogenesis. However, 5 days of running was able to re-establish NSC recruitment rate and to stimulate proliferation of $Nestin^+$ and DCX^+ progenitors up to levels largely exceeding physiological values detected in the p21 WT group.

Altogether, our findings reveal a previously unexplored link between physical activity, the genetic regulation of SVZ neurogenesis and olfactory behavior, mediated by modifications of the cell cycle, and the enhanced rate of new neurons maturation and functional integration in the pre-existing olfactory circuits. The crucial role of physical activity for neurogenic processes in the adult brain has been recently highlighted by the findings that in motor-deprived animals, a strong reduction of proliferation and differentiation in adult subventricular NSCs occurred [72]. Further analyses will lead to a deeper characterization of the molecular mechanisms underpinning the enduring self-renewal capacity of p21-null NSCs, with the ultimate goal of exploiting them as a potential source of active NSCs able to repair brain damage or counteract neurodegenerative processes.

Acknowledgements This work was supported by Regione Lazio Project FILAS to Stefano Farioli Vecchioli.

References

1. Katsimpardi L, Lledo PM (2018) Regulation of neurogenesis in the adult and aging brain. Curr Opin Neurobiol 53:131–138
2. Toda T, Parylak SL, Linker SB, Gage FH (2019) The role of adult hippocampal neurogenesis in brain health and disease. Mol Psychiatry 24(1):67–87
3. Anacker C, Luna VM, Stevens GS, Millette A, Shores R, Jimenez JC, Chen B, Hen R (2018) Hippocampal neurogenesis confers stress resilience by inhibiting the ventral dentate gyrus. Nature 559(7712):98–102
4. Eisinger BE, Zhao X (2018) Identifying molecular mediators of environmentally enhanced neurogenesis. Cell Tissue Res 371(1):7–21
5. Saraulli D, Costanzi M, Mastrorilli V, Farioli-Vecchioli S (2017) The long run: neuroprotective effects of physical exercise on adult neurogenesis from youth to old age. Curr Neuropharmacol 15(4): 519–533
6. Farioli Vecchioli S, Sacchetti S, Nicolis di Robilant V, Cutuli D (2018) The role of physical exercise and omega-3 fatty acids in depressive illness in the elderly. Curr Neuropharmacol 16(3):308–306
7. Hardy D, Saghatelyan A (2017) Different forms of structural plasticity in the adult olfactory bulb. Neurogenesis 4(1):e1301850
8. Alonso M, Lepousez G, Sebastien W, Bardy C, Gabellec MM, Torquet N, Lledo PM (2012) Activation of adult-born neurons facilitates learning and memory. Nat Neurosci 15(6):897–904
9. Shohayeb B, Diab M, Ahmed M, Ng DHC (2018) Factors that influence adult neurogenesis as potential therapy. Transl Neurodegener 7:4
10. Doetsch F, Caillé I, Lim DA, García-Verdugo JM, Alvarez-Buylla A (1999) Subventricular zone astrocytes are neural stem cells in the adult mammalian brain. Cell 97(6):703–716
11. Laywell ED, Rakic P, Kukekov VG, Holland EC, Steindler DA (2000) Identification of a multipotent astrocytic stem cell in the immature and adult mouse brain. Proc Natl Acad Sci U S A 97(25):13883–13888
12. Imura T, Kornblum HI, Sofroniew MV (2003) The predominant neural stem cell isolated from postnatal and adult forebrain but not early embryonic forebrain expresses GFAP. J Neurosci 23(7): 2824–2832
13. Urbán N, Guillemot F (2014) Neurogenesis in the embryonic and adult brain: same regulators, different roles. Front Cell Neurosci 27:396
14. Lim DA, Alvarez-Buylla A (2016) The adult ventricular-subventricular zone (V-SVZ) and olfactory bulb (OB) neurogenesis. Cold Spring Harb Perst Biol 8:a018820
15. Kosaka K, Aika Y, Toida K, Heizmann CW, Hunziker W, Jacobowitz DM, Nagatsu I, Streit P et al (1995) Chemically defined neuron groups and their subpopulations in the glomerular layer of the rat main olfactory bulb. Neurosci Res 23(1):73–88
16. Saghatelyan A, Carleton A, Lagier S, de Chevigny A, Lledo PM (2003) Local neurons play key roles in the mammalian olfactory bulb. J Physiol Paris 7(4–6):517–528
17. Kohwi M, Osumi N, Rubenstein JL, Alvarez-Buylla A (2005) Pax6 is required for making specific subpopulations of granule and periglomerular neurons in the olfactory bulb. J Neurosci 25(30): 6997–7003
18. Rochefort C, Gheusi G, Vincent JD, Lledo PM (2002) Enriched odor exposure increases the number of newborn neurons in the adult olfactory bulb and improves odor memory. J Neurosci 22(7):2679–2689
19. Zhao C, Deng W, Gage FH (2008) Mechanisms and functional implications for adult neurogenesis. Cell 132(4):645–660

20. Llorens-Bobadilla E, Zhao S, Baser A, Saiz-Castro G, Zwadlo K, Martin-Villalba A (2015) Single-cell transcriptomics reveals a population of dormant neural stem cells that become activated upon brain injury. Cell Stem Cell 17(3):329–340
21. Otsuki L, Brand AH (2018) Cell cycle heterogeneity directs the timing of neural stem cell activation from quiescence. Science 360(6384):99–102
22. Engler A, Rolando C, Giachino C, Saotome I, Erni A, Brien C, Zhang R, Zimber-Strobl U et al (2018) Notch2 signaling maintains NSC quiescence in the murine ventricular-subventricular zone. Cell Rep 22(4):992–1002
23. Sherr CJ, Roberts JM (1999) CDK inhibitors: positive and negative regulators of G1-phase progression. Genes Dev 13(12):1501–1512
24. Coqueret O (2003) New roles for p21 and p27 cell-cycle inhibitors: a function for each cell compartment? Trends Cell Biol 13(2):65–70
25. Gartel AL, Radhakrishnan SK (2005) Lost in transcription: p21 repression, mechanisms, and consequences. Cancer Res 65(10): 3980–3985
26. Rane CK, Minden A (2014) P21 activated kinases: structure, regulation, and functions. Small GTPases 5:e28003
27. Karimian A, Ahmadi Y, Yousefi B (2016) Multiple functions of p21 in cell cycle, apoptosis and transcriptional regulation after DNA damage. DNA Repair (Amst) 42:63–71
28. Pechnick RN, Chesnokova V (2009) Adult neurogenesis, cell cycle and drug discovery in psychiatry. Neuropsychopharmacology 34(1):244
29. Zonis S, Ljubimov VA, Mahgerefteh M, Pechnick RN, Wawrowsky K, Chesnokova V (2013) p21Cip restrains hippocampal neurogenesis and protects neuronal progenitors from apoptosis during acute systemic inflammation. Hippocampus 23(12):1383–1394
30. Farioli-Vecchioli S, Tirone F (2015) Control of the cell cycle in adult neurogenesis and its relation with physical exercise. Brain Plast 1(1):41–54
31. Qiu J, Takagi Y, Harada J, Rodrigues N, Moskowitz MA, Scadden D, Cheng T (2004) Regenerative response in ischemic brain restricted by p21cip1/waf1. J Exp Med 199(7):937–945
32. Porlan E, Morante-Redolat JM, Marqués-Torrejón MÁ, Andreu-Agulló C, Carneiro C, Gómez-Ibarlucea E, Soto A, Vidal A et al (2013) Transcriptional repression of Bmp2 by p21(Waf1/Cip1) links quiescence to neural stem cell maintenance. Nat Neurosci 16(11):1567–1575
33. Marqués-Torrejón MÁ, Porlan E, Banito A, Gómez-Ibarlucea E, Lopez-Contreras AJ, Fernández-Capetillo O, Vidal A, Gil J et al (2013) Cyclin-dependent kinase inhibitor p21 controls adult neural stem cell expansion by regulating Sox2 gene expression. Cell Stem Cell 12(1):88–100
34. van Praag H, Kempermann G, Gage FH (1999) Running increases cell proliferation and neurogenesis in the adult mouse dentate gyrus. Nat Neurosci 2(3):266–270
35. Kempermann G, Fabel K, Ehninger D, Babu H, Leal-Galicia P, Garthe A, Wolf SA (2010) Why and how physical activity promotes experience-induced brain plasticity. Front Neurosci 8:189
36. Vivar C, Potter MC, van Praag H (2013) All about running: synaptic plasticity, growth factors and adult hippocampal neurogenesis. Curr Top Behav Neurosci 15:189–210
37. Zhao Z, Sabirzhanov B, Wu J, Faden AI, Stoica BA (2015) Voluntary exercise preconditioning activates multiple antiapoptotic mechanisms and improves neurological recovery after experimental traumatic brain injury. J Neurotrauma 32(17):1347–1360
38. Archer T, Fredriksson A (2012) Delayed exercise-induced functional and neurochemical partial restoration following MPTP. Neurotox Res 21(2):210–221
39. Piao CS, Stoica BA, Wu J, Sabirzhanov B, Zhao Z, Cabatbat R, Loane DJ, Faden AI (2013) Late exercise reduces neuroinflammation and cognitive dysfunction after traumatic brain injury. Neurobiol Dis 54:252–263
40. Brown J, Cooper-Kuhn CM, Kempermann G, Van Praag H, Winkler J, Gage FH, Kuhn HG (2003) Enriched environment and physical activity stimulate hippocampal but not olfactory bulb neurogenesis. Eur J Neurosci 17(10):2042–2046
41. Bednarczyk MR, Aumont A, Décary S, Bergeron R, Fernandes KJ (2009) Prolonged voluntary wheel-running stimulates neural precursors in the hippocampus and forebrain of adult CD1 mice. Hippocampus 19(10):913–927
42. Blackmore DG, Vukovic J, Waters MJ, Bartlett PF (2012) GH mediates exercise-dependent activation of SVZ neural precursor cells in aged mice. PLoS One 7(11):e49912
43. Lee JC, Yau SY, Lee TMC, Lau BW, So KF (2016) Voluntary wheel running reverses the decrease in subventricular zone neurogenesis caused by corticosterone. Cell Transplant 25(11): 1979–1986
44. Mastrorilli V, Scopa C, Saraulli D, Costanzi M, Scardigli R, Rouault JP, Farioli-Vecchioli S, Tirone F (2017) Physical exercise rescues defective neural stem cells and neurogenesis in the adult subventricular zone of Btg1 knockout mice. Brain Struct Funct 222(6):2855–2876
45. Farioli-Vecchioli S, Mattera A, Micheli L, Ceccarelli M, Leonardi L, Saraulli D, Costanzi M, Cestari V et al (2014) Running rescues defective neurogenesis by shortening the length of the cell cycle of neural stem and progenitor cells. Stem Cells 32(7):1968–1982
46. Brugarolas J, Chandrasekaran C, Gordon JI, Beach D, Jacks T, Hannon GJ (1995) Radiation-induced cell cycle arrest compromised by p21 deficiency. Nature 377(6549):552–557
47. Farioli-Vecchioli S, Micheli L, Saraulli D, Ceccarelli M, Cannas S, Scardigli R, Leonardi L, Cinà I et al (2012) Btg1 is required to maintain the pool of stem and progenitor cells of the dentate gyrus and subventricular zone. Front Neurosci 6:124
48. Mignone JL, Kukekov V, Chiang AS, Steindler D, Enikolopov G (2004) Neural stem and progenitor cells in nestin-GFP transgenic mice. J Comp Neurol 469(3):311–324
49. Colak D, Mori T, Brill MS, Pfeifer A, Falk S, Deng C, Monteiro R, Mummery C et al (2008) Adult neurogenesis requires Smad4-mediated bone morphogenic protein signaling in stem cells. J Neurosci 28(2):434–446
50. Brandt MD, Hübner M, Storch A (2012) Brief report: adult hippocampal precursor cells shorten S-phase and total cell cycle length during neuronal differentiation. Stem Cells 30(12):2843–2847
51. Cryan JF, Sweeney FF (2011) The age of anxiety: role of animal models of anxiolytic action in drug discovery. Br J Pharmacol 164(4):1129–1161
52. Markel AL, Galaktionov YK, Efimov VM (1989) Factor analysis of rat behavior in an open field test. Neurosci Behav Physiol 19(4): 279–286
53. Breton-Provencher V, Lemasson M, Peralta MR 3rd, Saghatelyan A (2009) Interneurons produced in adulthood are required for the normal functioning of the olfactory bulb network and for the execution of selected olfactory behaviors. J Neurosci 29(48):15245–15257
54. Wang W, Lu S, Li T, Pan YW, Zou J, Abel GM, Xu L, Storm DR et al (2015) Inducible activation of ERK5 MAP kinase enhances adult neurogenesis in the olfactory bulb and improves olfactory function. J Neurosci 35(20):7833–7849
55. Kippin TE, Martens DJ, van der Kooy D (2005) p21 loss compromises the relative quiescence of forebrain stem cell proliferation leading to exhaustion of their proliferation capacity. Genes Dev 19(6):756–767
56. Sakamoto M, Ieki N, Miyoshi G, Mochimaru D, Miyachi H, Imura T, Yamaguchi M, Fishell G et al (2014) Continuous postnatal neurogenesis contributes to formation of the olfactory bulb neural

circuits and flexible olfactory associative learning. J Neurosci 34(17):5788–5799
57. Yamaguchi M, Manabe H, Murata K, Mori K (2013) Reorganization of neuronal circuits of the central olfactory system during postprandial sleep. Front Neural Circuits 7:132
58. Veyrac A, Sacquet J, Nguyen V, Marien M, Jourdan F, Didier A (2009) Novelty determines the effects of olfactory enrichment on memory and neurogenesis through noradrenergic mechanisms. Neuropsychopharmacology 34(3):786–795
59. Sultan S, Rey N, Sacquet J, Mandairon N, Didier A (2011) Newborn neurons in the olfactory bulb selected for long-term survival through olfactory learning are prematurely suppressed when the olfactory memory is erased. J Neurosci 31(42):14893–14898
60. Bragado Alonso S, Reinert JK, Marichal N, Massalini S, Berninger B, Kuner T, Calegari F (2019) An increase in neural stem cells and olfactory bulb adult neurogenesis improves discrimination of highly similar odorants. EMBO J 38(6):e98791
61. Salomoni P, Calegari F (2010) Cell cycle control of mammalian neural stem cells: putting a speed limit on G1. Trends Cell Biol 20(5):233–243
62. Lange C, Calegari F (2010) Cdks and cyclins link G1 length and differentiation of embryonic, neural and hematopoietic stem cells. Cell Cycle 9(10):1893–1900
63. Artegiani B, Lindemann D, Calegari F (2011) Overexpression of cdk4 and cyclinD1 triggers greater expansion of neural stem cells in the adult mouse brain. J Exp Med 208(5):937–948
64. Fasano CA, Dimos JT, Ivanova NB, Lowry N, Lemischka IR, Temple S (2007) shRNA knockdown of Bmi-1reveals a critical role for p21-Rb pathway in NSC self-renewal during development. Cell Stem Cell 1(1):87–99
65. Li W, Sun G, Yang S, Qu Q, Nakashima K, Shi Y (2008) Nuclear receptor TLX regulates cell cycle progression in neural stem cells of the developing brain. Mol Endocrinol 22(1):56–64
66. Heldring N, Joseph B, Hermanson O, Kioussi C (2012) Pitx2 expression promotes p21 expression and cell cycle exit in neural stem cells. CNS Neurol Disord Drug Targets 11(7):884–892
67. Xu H, Wang Z, Jin S, Hao H, Zheng L, Zhou B, Zhang W, Lv H et al (2014) Dux4 induces cell cycle arrest at G1 phase through upregulation of p21 expression. Biochem Biophys Res Commun 446(1):235–240
68. Sakamoto M, Kageyama R, Imayoshi I (2014) The functional significance of newly born neurons integrated into olfactory bulb circuits. Front Neurosci 8:121
69. Enwere E, Shingo T, Gregg C, Fujikawa H, Ohta S, Weiss S (2004) Aging results in reduced epidermal growth factor receptor signaling, diminished olfactory neurogenesis, and deficits in fine olfactory discrimination. J Neurosci 24(38):8354–8365
70. Pan YW, Kuo CT, Storm DR, Xia Z (2012) Inducible and targeted deletion of the ERK5 MAP kinase in adult neurogenic regions impairs adult neurogenesis in the olfactory bulb and several forms of olfactory behavior. PLoS One 7(11):e49622
71. Mastrodonato A, Barbati SA, Leone L, Colussi C, Gironi K, Rinaudo M, Piacentini R, Denny CA et al (2018) Olfactory memory is enhanced in mice exposed to extremely low-frequency electromagnetic fields via Wnt/β-catenin dependent modulation of subventricular zone neurogenesis. Sci Rep 8(1):262
72. Adami R, Pagano J, Colombo M, Platonova N, Recchia D, Chiaramonte R, Bottinelli R, Canepari M et al (2018) Reduction of movement in neurological diseases: effects on neural stem cells characteristics. Front Neurosci 12:336